Inorg. Chem. **2009**, *48*, 978−990

Mixed-Metal Assemblies Involving Ferrocene−Naphthyridine Hybrids

Nabanita Sadhukhan and Jitendra K. Bera*

Department of Chemistry, Indian Institute of Technology Kanpur, Kanpur 208 016, India

Received August 20, 2008

Covalent attachment of one and two NP moieties to a ferrocenyl unit provides organometallic ligands 1,8-naphthyrid-2-yl-ferrocene (FcNP) and 1,1′-bis(1,8-naphthyrid-2-yl)ferrocene ($FcNP_2$). Coordination of FcNP to transition metal ions Fe^{II}, Cu^{II}, Zn^{II}, and Cd^{II} provides $[FeCl_2(\kappa N_8\text{-FcNP})_2]$ (**1**), $[Cu(\kappa N_8\text{-FcNP})_2(NO_3)_2]$ (**2**), $[Zn(\kappa N_8\text{-FcNP})_4][OTf]_2$ (**3**), and $[Cd(\kappa N_8\text{-FcNP})_2(\kappa^2 N_1,N_8\text{-FcNP})_2][BF_4]_2$ (**4**), respectively. Dirhodium(II) compound $[Rh_2(\mu\text{-FcNP})_2(\mu\text{-}O_2CCH_3)_2(H_2O)][OTf]_2$ (**5**) is isolated when acetonitrile-solvated $[Rh_2(\mu\text{-}O_2CCH_3)_2]^{2+}$ is employed as a precursor. Diverse bonding modes of the NP unit, including monodentate, bidentate chelating, or binuclear bridging, are revealed in these FcNP clusters. Metallamacrocycles $[M_2(FcNP_2)_2][X]_2$ (M = Cu, X = ClO_4 (**6**); M = Ag, X = OTf (**7**)), $[PdCl_2(FcNP_2)]$ (**8**), and $[ZnCl_2(FcNP_2)]_4$ (**10**) are obtained by the reaction of $CuClO_4$, AgOTf, $Pd(C_6H_5CN)_2Cl_2$, and $ZnCl_2$ with $FcNP_2$ in 1:1 ratios. Treatment of Cu^{I} and $FcNP_2$ in a 2:1 ratio provides $[Cu_2(FcNP_2)][ClO_4]_2$ (**9**). Molecular structures of compounds **1**−**10** have been determined by X-ray diffraction studies. Interconversion between 1:1 dimer **6** and 2:1 dimer **9** occurs by the addition of a requisite amount of Cu^{I} or $FcNP_2$. ESI-MS experiments reveal that the predominant species is the 1:1 complex $\{Cu(FcNP_2)\}^{1+}$ in solution for both **6** and **9**. Synthesis, structures, mass spectroscopy, and electrochemistry of the transition metal compounds of FcNP and $FcNP_2$ are discussed.

Introduction

The quest to create novel molecular architectures, to a large extent, has motivated the growth of inorganic supramolecular chemistry.[1] The prospect, however, lies on their ability to function as useful materials.[2] Ferrocene-based compounds are most promising, as reflected in their increasing role in industry, material chemistry, and biology.[3] The incorporation of heteroatomic units, such as pyridine,[4] pyrazine,[5] pyrimidine,[5] thiophene,[6] quinolene,[7] imidazole,[8] triazole,[8] pyrazole,[9] thiazole,[10] bipyridine,[11] and terpyridine,[12] linked directly or through molecular spacers, rigid and flexible, resulted in a series of organometallic ligands. Transition metal compounds of these ligands have found wider application, for example, as polymerization catalysts,[13] chiral catalysts,[14] molecular receptors,[15] materials for nonlinear optics,[16] molecular magnets,[17] and antitumor agents.[18]

We are involved in the construction of mixed-metal assemblies by the complexation of ferrocene-based ligands with transition metal ions. The demonstrated ability of the 1,8-naphthyridine (NP) unit to bind metal ion(s) in different modes, including monodentate,[19] bidentate chelating,[20] or

* Author to whom correspondence should be addressed. Phone: +91-512-259 7336. Fax: +91-512-259 7436. E-mail: jbera@iitk.ac.in.

(1) (a) Lehn, J.-M. *Supramolecular Chemistry—Concepts and Perspectives*; VCH: Weinheim, Germany, 1995. (b) *Comprehensive Supramolecular Chemistry*; Atwood, J. L., Davies, J. E. D., MacNicol, D. D., Vögtle, F., Lehn, J.-M., Eds.; Pergamon, Oxford, 1996; Vol. 9. (c) Bera, J. K.; Bacsa, J.; Dunbar, K. R. *Encyclopedia of Inorganic Chemistry*, 2nd ed.; King, B. R., Ed.; John Wiley & Sons, Inc.: New York, 2005. (d) Videnova-Adrabinska, V. *Coord. Chem. Rev.* **2007**, *251*, 1987. (e) Gale, P. A.; Quesada, R. *Coord. Chem. Rev.* **2006**, *250*, 3219. (f) Ruben, M.; Lehn, J.-M.; Müller, P. *Chem. Soc. Rev.* **2006**, *35*, 1056. (g) Keizer, H. M.; Sijbesma, R. P. *Chem. Soc. Rev.* **2005**, *34*, 226. (h) Sieklucka, B.; Podgajny, R.; Przychodzeń, P.; Korzeniak, T. *Coord. Chem. Rev.* **2005**, *249*, 2203. (i) Kawano, M.; Fujita, M. *Coord. Chem. Rev.* **2007**, *251*, 2592. (j) Fujita, M. *Chem. Soc. Rev.* **1998**, *27*, 417. (k) Fujita, M. *Acc. Chem. Res.* **1999**, *32*, 53. (l) Fujita, M.; Ogura, K. *Coord. Chem. Rev.* **1996**, *148*, 249.

(2) (a) Elhabiri, M.; Albrecht-Gary, A.-M. *Coord. Chem. Rev.* **2008**, *252*, 1079. (b) Friese, V. A.; Kurth, D. G. *Coord. Chem. Rev.* **2008**, *252*, 199. (c) Hembury, G. A.; Borovkov, V. V.; Inoue, Y. V. *Chem. Rev.* **2008**, *108*, 1. (d) Descalzo, A. B.; Martínez-Máñez, R.; Sancenón, F.; Hoffmann, K.; Rurack, K. *Angew. Chem., Int. Ed.* **2006**, *45*, 5924. (e) Waldmann, O. *Coord. Chem. Rev.* **2005**, *249*, 2550. (f) Thanasekarana, P.; Liao, R.-T.; Liu, Y.-H.; Rajendran, T.; Rajagopal, S.; Lu, K.-L. *Coord. Chem. Rev.* **2005**, *249*, 1085. (g) Beer, P. D.; Gale, P. A. *Angew. Chem., Int. Ed.* **2001**, *40*, 486.

(3) (a) Long, N. J. *Metallocenes: An Introduction to Sandwich Complexes*; Blackwell Science, Inc.: Cambridge, MA, 1998. (b) Fihri, A.; Meunir, P.; Hierso, J.-C. *Coord. Chem. Rev.* **2007**, *251*, 2017. (c) Staveren, D. R. V.; Metzler-Nolte, N. *Chem. Rev.* **2004**, *104*, 5931. (d) Colacot, T. J. *Chem. Rev.* **2003**, *103*, 3101. (e) Nguyen, P.; Gomej-Elipe, P.; Manners, I. *Chem. Rev.* **1999**, *99*, 1515.

10.1021/ic801586d CCC: $40.75
Published on Web 12/23/2008

binuclear bridging,[21] as shown in Chart 1, and the conformational flexibility of the ferrocenyl rings, illustrated by different conformers[22] in Chart 2, prompted the utilization of Fc−NP hybrids in building self-assembled inorganic architectures. Covalent attachments of one and two NP moieties to the ferrocenyl unit provide the organometallic ligands 1,8-naphthyrid-2-yl-ferrocene (FcNP) and 1,1′-bis(1,8-naphthyrid-2-yl)ferrocene ($FcNP_2$), respectively, the structures of which are depicted in Scheme 1.[23]

Chart 1. Possible Coordination Modes of the Naphthyridine (NP) Unit

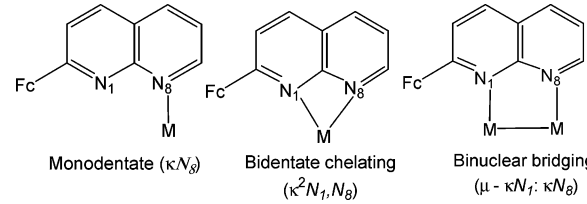

The FcNP ligand, on complexation with transition metal ions, provides a variety of ferrocene clusters, and metal-

(4) (a) Braga, D.; Polito, M.; Bracaccini, M.; D'Addario, D.; Tagliavini, E.; Proserpio, D. M.; Grepioni, F. *Chem. Commun.* **2002**, 1080. (b) Chen-jie, F.; Chun-ying, D.; Dong, G.; Cheng, H.; Qing-jin, M.; Zheming, W.; Chun-hua, Y. *Chem. Commun.* **2001**, 2540. (c) Horikoshi, R.; Mochida, T.; Moriyama, H. *Inorg. Chem.* **2002**, *41*, 3017. (d) Braga, D.; Polito, M.; D'Addario, D.; Tagliavini, E.; Proserpio, D. M.; Grepioni, F.; Steed, J. W. *Organometallics* **2003**, *22*, 4532. (e) Braga, D.; Polito, M.; Bracaccini, M.; D'Addario, D.; Tagliavini, E.; Sturba, L. *Organometallics* **2003**, *22*, 2142. (f) Chen-jie, F.; Chun-ying, D.; Hong, M.; Cheng, H.; Qing-jin, M.; Yong-jiang, L.; Yu-hua, M.; Zheming, W. *Organometallics* **2001**, *20*, 2525. (g) Barranco, E. M.; Crespo, O.; Gimeno, M. C.; Jones, P. G.; Laguna, A.; Sarroca, C. *J. Chem. Soc., Dalton Trans.* **2001**, 2523. (h) Gibson, V. C.; Halliwell, C. M.; Long, N. J.; Oxford, P. J.; Smith, A. M.; White, A. J. P.; Williams, D. J. *Dalton Trans.* **2003**, 918. (i) Lindner, E.; Zong, R.; Eichele, K.; Weisser, U.; Ströbele, M. *Eur. J. Inorg. Chem.* **2003**, 705. (j) Tani, K.; Mihana, T.; Yamagata, T.; Saito, T. *Chem. Lett.* **1991**, 2047. (k) Xue, W.-M.; Kühn, F. E.; Herdtweck, E.; Li, Q. *Eur. J. Inorg. Chem.* **2001**, 213.

(5) (a) Horikoshi, R.; Nambu, C.; Mochida, T. *Inorg. Chem.* **2003**, *42*, 6868. (b) Braga, D.; D'Addario, D.; Polito, M. *Organomeallics* **2004**, *23*, 2810. (c) Paolucci, D.; Marcaccio, M.; Bruno, C.; Braga, D.; Polito, M.; Paolucci, F.; Grepioni, F. *Organometallics* **2005**, *24*, 1198.

(6) (a) Zhu, Y.; Wolf, M. O. *J. Am. Chem. Soc.* **2000**, *122*, 10121. (b) Thomas, K. R. J.; Lin, J. T.; Wen, Y. S. *Organometallics* **2000**, *19*, 1008. (c) Wong, W.-Y.; Lu, G.-L.; Ng, K.-F.; Choi, K.-H.; Lin, Z. *J. Chem. Soc., Dalton Trans.* **2001**, 3250. (d) Thomas, K. R. J.; Lin, J. T.; Wen, Y. S. *J. Organomet. Chem.* **1999**, *575*, 301. (e) Pannell, K. H.; Wang, F.; Sharma, H. K.; Cervantes-Lee, F. *Polyhedron* **2000**, *19*, 291.

(7) (a) Enders, M.; Kohl, G.; Pritzkow, H. *Organometallics* **2002**, *21*, 1111. (b) Enders, M.; Ludwig, G.; Pritzkow, H. *Organometallics* **2002**, *21*, 3856. (c) Liu, C.-M.; Chen, B.-H.; Liu, W.-Y.; Wu, X.-L.; Ma, Y.-X. *J. Organomet. Chem.* **2000**, *598*, 348. (d) Enders, M.; Kohl, G.; Pritzkow, H. *J. Organomet. Chem.* **2001**, *622*, 66. (e) Mamane, V.; Fort, Y. *J. Org. Chem.* **2005**, *70*, 8220.

(8) (a) Gao, Y.; Twamley, B.; Shreeve, J. M. *Organometallics* **2006**, *25*, 3364. (b) Badèche, S.; Daran, J.-C.; Ruiz, J.; Astruc, D. *Inorg. Chem.* **2008**, *47*, 4903.

(9) (a) Reger, D. L.; Brown, K. J.; Gardinier, J. R.; Smith, M. D. *Organometallics* **2003**, *22*, 4973. (b) Guo, S. L.; Peters, F.; Fabrizi de Biani, F.; Bats, J. W.; Herdtweck, E.; Zanello, P.; Wagner, M. *Inorg. Chem.* **2001**, *40*, 4928. (c) Dinnebier, R. E.; Ding, L.; Ma, K.; Neumann, M. A.; Tanpipat, N.; Leusen, F. J. J.; Stephens, W. P.; Wagner, M. *Organometallics* **2001**, *20*, 5642. (d) Biani, F. F. D.; Jäkle, F.; Spiegler, M.; Wagner, M.; Zanello, P. *Inorg. Chem.* **1997**, *36*, 2103. (e) Reger, D. L.; Brown, K. J.; Gardinier, J. R.; Smith, M. D. *J. Organomet. Chem.* **2005**, *690*, 1889. (f) Ilkhechi, A. H.; Bolte, M.; Lerner, H. W.; Wagner, M. *J. Organomet. Chem.* **2005**, *690*, 1971. (g) Herdtweck, E.; Peters, F.; Scherer, W.; Wagner, M. *Polyhedron* **1998**, *17*, 1149. (h) Carrion, M. C.; Diaz, A.; Guerrero, A.; Jalon, F. A.; Manzano, B. R.; Rodriguez, A. *New J. Chem.* **2002**, *26*, 305.

(10) Caballero, A.; Lioveras, V.; Curiel, D.; Tárraga, A.; Espinosa, A.; Garcia, R.; Vidal-Gancedo, J.; Rovira, C.; Wurst, K.; Molina, P.; Veciana, J. *Inorg. Chem.* **2007**, *46*, 825.

(11) (a) Ion, A.; Moutet, J.-C.; Saint-Amam, E.; Royal, G.; Tingry, S.; Pecaut, J.; Menage, S.; Ziessel, R. *Inorg. Chem.* **2001**, *40*, 3632. (b) Buda, M.; Moutet, J.-C.; Saint-Aman, E.; Cian, A. D.; Fischer, J.; Ziessel, R. *Inorg. Chem.* **1998**, *37*, 4146. (c) Packheiser, R.; Walfort, B.; Lang, H. *Organometallics* **2006**, *25*, 4579. (d) Beer, P. D.; Kocian, O.; Mortimer, R. J. *J. Chem. Soc., Dalton Trans.* **1990**, 3283. (e) Butler, I. R. *Organometallics* **1992**, *11*, 74. (f) Sachsinger, N.; Hall, C. D. *J. Organomet. Chem.* **1997**, *531*, 61. (g) König, B.; Nimtz, M.; Zieg, H. *Tetrahedron* **1995**, *51*, 6267; and references therein.

(12) (a) Siemeling, U.; Brüggen, J. V. D.; Vorfeld, U.; Neumann, B.; Stammler, A.; Stamler, H.-G.; Brockhinke, A.; Plessow, R.; Zanello, P.; Laschi, F.; Biani, F. F. D.; Fontani, M.; Steenken, S.; Stapper, M.; Gurzadyn, G. *Chem.—Eur. J.* **2003**, *9*, 2819. (b) Dong, T.-Y.; Chen, K.; Lin, M.-C.; Lee, L. *Organometallics* **2005**, *24*, 4198. (c) Dong, T.-Y.; Lin, M.-C.; Chiang, M. Y.-N.; Wu, J.-Y. *Organometallics* **2004**, *23*, 3921. (d) Dong, T.-Y.; Lin, M.-C.; Chiang, M. Y.-N. *Inorg. Chem. Commun.* **2004**, *7*, 687. (e) Constable, E. C.; Edwards, A. J.; Marcos, M. D.; Raithby, P. R.; Martínez-Máñez, R.; Tendero, M. J. L. *Inorg. Chim. Acta* **1994**, *224*, 11.

(13) (a) Gregson, C. K. A.; Gibson, V. C.; Long, N. J.; Marshall, E. L.; Oxford, P. J.; White, A. J. P. *J. Am. Chem. Soc.* **2006**, *128*, 7410. (b) Shafir, A.; Arnold, J. *Organometallics* **2003**, *22*, 567. (c) Honeyman, G. W.; Kennedy, A. R.; Mulvey, R. E.; Sherrington, D. C. *Organometallics* **2004**, *23*, 1197. (d) Weng, Z.; Teo, S.; Andy Hor, T. S. *Organometallics* **2006**, *25*, 4878. (e) Gibson, V. C.; Long, N. J.; Oxford, P. J.; White, A. J. P.; Williams, D. J. *Organometallics* **2006**, *25*, 1932. (f) Atkinson, R. C. J.; Gerry, K.; Gibson, V. C.; Long, N. J.; Marshall, E. L.; West, L. J. *Organometallics* **2007**, *26*, 316. (g) Eppinger, J.; Nikolaides, K. R.; Zhang-Presse, M.; Riederer, F. A.; Rabe, G. W.; Rheingold, A. L. *Organometallics* **2008**, *27*, 736. (h) Wang, T.; Chen, J. W.; Li, Z. Q.; Wan, P. Y. *J. Photochem. Photobiol. A, Chem.* **2007**, *187*, 389.

(14) (a) Dai, L.-X.; Tu, T.; You, S.-L.; Deng, W.-P.; Hou, X.-L. *Acc. Chem. Res.* **2003**, *36*, 659. (b) Chen, W.; Mbafor, W.; Roberts, M. S.; Whittall, J. *J. Am. Chem. Soc.* **2006**, *128*, 3922. (c) Bolm, C.; Rudolph, J. *J. Am. Chem. Soc.* **2002**, *124*, 14850. (d) Mancheño, O. G.; Arrayás, R. G.; Carretero, J. C. *J. Am. Chem. Soc.* **2004**, *126*, 456. (e) Takai, I.; Nishibayashi, Y.; Ishii, Y.; Mizobe, Y.; Uemura, S.; Hidai, M. *Chem. Commun.* **2001**, 2360. (f) Deng, W.-P.; Hou, X.-L.; Dai, L.-X.; Dong, X.-W. *Chem, Commun.* **2000**, 1483. (g) Bolm, C.; Muñiz, K. *Chem. Commun.* **1999**, 1295. (h) Bolm, C.; Muñiz, K.; Hildebrand, J. P. *Org. Lett.* **1999**, *1*, 491. (i) Hoang, V. D. M.; Reddy, P. A. N.; Kim, T.-J. *Organometallics* **2008**, *27*, 1026. (j) Bianchini, C.; Meli, A.; Oberhouser, W.; Parisel, S. *Organometallics* **2005**, *24*, 1018. (k) Bianchini, C.; Oberhouser, W.; Orlandini, A. *Organometallics* **2005**, *24*, 3692. (l) Tu, T.; Zhou, Y.-G.; Hou, X.-L.; Dai, L.-X.; Dong, X.-C.; Yu, Y.-H.; Sun, J. *Organometallics* **2003**, *22*, 1255. (m) Brunker, T. J.; Moncarz, J. R.; Glueck, D. S.; Zakharov, L. N.; Golen, J. A.; Rheingold, A. L. *Organometallics* **2004**, *23*, 2228. (n) Weng, Z.; Teo, S.; Koh, L. L.; Hor, T. S. A. *Organometallics* **2004**, *23*, 3603. (o) Kim, T.-J.; Lee, H.-Y.; Ryu, E.-S.; Park, D.-K.; Cho, C. S.; Shim, S. C.; Jeong, J. H. *J. Organomet. Chem.* **2002**, *649*, 258. (p) Tu, T.; Hou, X.-L.; Dai, L.-X. *J. Organomet. Chem.* **2004**, *689*, 3847. (q) Mancheño, O. G.; Priego, J.; Cabrera, S.; Arrayás, R. G.; Llamas, T.; Carretero, J. C. *J. Org. Chem.* **2003**, *68*, 3679.

(15) (a) Beer, P. D. *Chem. Commun.* **1996**, 689. (b) Otón, F.; Espinosa, A.; Tárraga, A.; Molina, P. *Organometallics* **2007**, *26*, 6234. (c) Westwood, J.; Coles, S. J.; Collinson, S. R.; Gasser, G.; Green, S. J.; Hursthouse, M. B.; Light, M. E.; Tucker, J. H. R. *Organometallics* **2004**, *23*, 946. (d) Beer, P. D.; Blackburn, T. C.; McAleer, J. F.; Sikanyika, H. *Inorg. Chem.* **1990**, *29*, 378. (e) Beer, P. D.; Graydon, A. R.; Johnson, A. O. M.; Smith, D. K. *Inorg. Chem.* **1997**, *36*, 2112. (f) Georgopoulou, A. S.; Mingos, D. M. P.; White, A. J. P.; Williams, D. J.; Horrocks, B. R.; Houlton, A. *J. Chem. Soc., Dalton Trans.* **2000**, 2969. (g) Kingston, J. E.; Ashford, L.; Beer, P. D.; Drew, G. B. *J. Chem. Soc., Dalton Trans.* **1999**, 251.

(16) (a) Long, N. J. *Angew. Chem., Int. Ed. Engl.* **1995**, *34*, 21. (b) Barlow, S.; Bunting, H. E.; Ringham, C.; Green, J. C.; Bublitz, G. U.; Boxer, S. G.; Perry, J. W.; Marder, S. R. *J. Am. Chem. Soc.* **1999**, *121*, 3715. (c) Li, G.; Song, Y. L.; Hou, H.; Li, L.; Fan, Y.; Zhu, Y.; Meng, X.; Mi, L. *Inorg. Chem.* **2003**, *42*, 913. (d) Jayaprakash, K. N.; Ray, P. C.; Matsuoka, I.; Bhadbhade, M. M.; Puranik, V. G.; Das, P. K.; Nishihara, H.; Sarkar, A. *Organometallics* **1999**, *18*, 3851. (e) Lee, I. S.; Seo, H.; Chung, Y. K. *Organometallics* **1999**, *18*, 1091. (f) Sharma, H. K.; Pannell, K. H.; Ledoux, I.; Zyss, J.; Ceccanti, A.; Zanello, P. *Organometallics* **2000**, *19*, 770. (g) Farrell, T.; Meyer-Friedrichsen, T.; Malessa, M.; Haase, D.; Saak, W.; Asselberghs, I.; Wostyn, K.; Clays, K.; Persoons, A.; Heck, J.; Manning, A. R. *J. Chem. Soc., Dalton Trans.* **2001**, 29. (h) Davies, D. A.; Silver, J.; Cross, G.; Thomas, P. J. *J. Organomet. Chem.* **2001**, *631*, 59.

Chart 2. Ideal Conformations of the Ferrocenyl Rings in 1,1′-Disubstituted Ferrocene

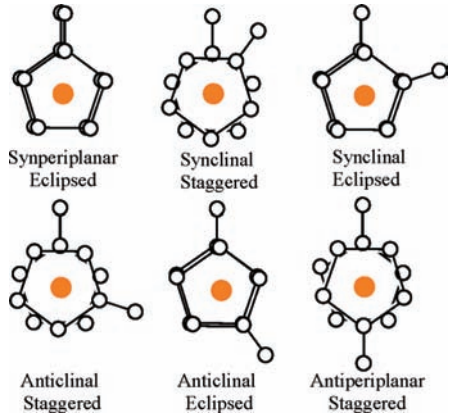

lamacrocycles are isolated with $FcNP_2$. Syntheses, structures, electrochemical studies of an assortment of mixed-metal compounds, and the interconversion between two topologically different copper(I)-based metallacycles are described in this paper.

Scheme 1. Line Drawings of FcNP and $FcNP_2$

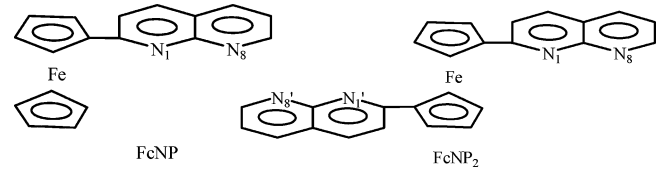

Results and Discussion

Mixed-Metal Complexes of FcNP. Since this study necessitates an intimate understanding of the coordination versatility of the NP unit, divalent metal ions are reacted with FcNP toward the isolation and structural characterization of mixed-metal compounds. Reactions of appropriate salts of Fe^{II}, Cu^{II}, Zn^{II}, and Cd^{II} provide $[FeCl_2(\kappa N_8\text{-FcNP})_2]$ (**1**), $[Cu(\kappa N_8\text{-FcNP})_2(NO_3)_2]$ (**2**), $[Zn(\kappa N_8\text{-FcNP})_4][OTf]_2$ (**3**), and $[Cd(\kappa N_8\text{-FcNP})_2(\kappa^2 N_1,N_8\text{-FcNP})_2][BF_4]_2$ (**4**). The bridged dirhodium(II) compound $[Rh_2(\mu\text{-FcNP})_2(\mu\text{-}O_2CCH_3)_2(H_2O)][OTf]_2$ (**5**) is isolated when $[Rh_2(\mu\text{-}O_2CCH_3)_2(CH_3CN)_6]^{2+}$ is employed as a precursor. Molecular structures of neutral and dicationic units of complexes **1**−**5** are depicted in Figure 1. Important metrical parameters are listed therein. In structure descriptions, we refer to the N_1 and N_8 atoms of FcNP and $FcNP_2$ (Scheme 1) as "proximal" and "distal" nitrogen, respectively. ESI-MS spectra of complexes **1**−**5** are provided in the Supporting Information (Figure S9a−e, Supporting Information).

In the neutral complex $[FeCl_2(\kappa N_8\text{-FcNP})_2]$ (**1**), two chlorine atoms and two FcNP ligands provide distorted tetrahedral geometry to the central iron atom. Each FcNP binds to the metal using distal nitrogen of the naphthyridine unit. The distances between the central iron atom and ligating nitrogen atoms are 2.064(2) and 2.095(2) Å. A large N1−Fe1−N3 angle (130.04(9)°) is attributed to the bulky ferrocene appendages. The Cl2−Fe1−Cl1 angle is 103.00(3)°, and N−Fe−Cl angles range from 102.55(7)° to 109.43(6)° (Figure 1a). In a related complex $[Fe(NP)_4]^{2+}$, the Fe−N distances vary over a large range from 2.178 to 2.756 Å, and two sets of N−Fe−N angles, ranging from 54.1° to 58.4° and 111.0° to 114.3° are reported.[20a] The ESI-MS spectrum of **1** exhibits a signal at *m*/*z* 719 corresponding to $[M - Cl]^+$.

The molecular structure of $[Cu(\kappa N_8\text{-FcNP})_2(NO_3)_2]$ (**2**) reveals four donor atoms coordinated to copper, within a radius of 2.5 Å or less, consisting of two distal nitrogen atoms from two cis FcNP ligands and two oxygen atoms from two cis nitrates. The Cu−N distances are 1.989(2) and 2.001(2) Å, and the Cu−O distances are 1.966(2) and 2.001(2) Å. The Cu1−N2, Cu1−N4, Cu1−O3, and Cu1−O6 distances, 2.646(2), 2.867(2), 2.772(2), and 2.659(2) Å, respectively, are too long to consider any interaction between the atoms in a pair (Figure 1b). The Cu1, N1, N3, and O1 atoms are coplanar, with an average deviation of 0.04 Å. The atom O4 lies 0.61 Å out of this plane. The angle between two coordinating nitrogen atoms and the central Cu atom is

(17) (a) Miller, J. S.; Epstein, A. J. *Angew. Chem., Int. Ed. Engl.* **1994**, *33*, 385. (b) Koivisto, B. D.; Ichimura, S. A.; McDonald, R.; Lemaire, M. T.; Thompson, L. K.; Hicks, R. G. *J. Am. Chem. Soc.* **2006**, *128*, 690. (c) Wang, G.; Slebodnick, C.; Butcher, R. J.; Tam, M. C.; Crawford, T. D.; Yee, G. T. *J. Am. Chem. Soc.* **2004**, *126*, 16890. (d) Gebert, E., Jr.; Miller, J. S.; Rommelmann, H.; Epstein, A. J. *J. Am. Chem. Soc.* **1982**, *104*, 4403. (e) Miller, J. S.; Calabrese, J. C.; Rommelmann, H.; Chittipeddi, S. R.; Zhang, J. H.; Reiff, W. M.; Epstein, A. J. *J. Am. Chem. Soc.* **1987**, *109*, 769. (f) Miller, J. S.; Epstein, A. J.; Reiff, W. M. *Chem. Rev.* **1988**, *88*, 201. (g) Hou, H.; Li, L.; Zhu, Y.; Fan, Y.; Qiao, Y. *Inorg. Chem.* **2004**, *43*, 4767. (h) Togni, A.; Hobi, M.; Rihs, G.; Rist, G.; Albinati, A.; Zanello, P.; Zech, D.; Keller, H. *Organometallics* **1994**, *13*, 1224. (i) Pullen, A. E.; Faulmann, C.; Pokhodnya, K. I.; Cassoux, P.; Tokumoto, M. *Inorg. Chem.* **1998**, *37*, 6714. (j) Hou, H.; Li, G.; Li, L.; Zhu, Yu.; Meng, X.; Yaoting, F. *Inorg. Chem.* **2003**, *42*, 428. (k) Schweizer, J.; Bencini, A.; Carbonera, C.; Epstein, A. J.; Golhen, S. E.; Lelie'vre-Berna, E.; Miller, J. S.; Ouahab, L.; Pontillon, Y.; Ressouche, E.; Zheludev, A. *Polyhedron* **2001**, *20*, 1771. (l) Narayan, K. S.; Epstein, A. J. *J. Appl. Phys.* **1991**, *69*, 5953. (m) Chakraborty, A.; Epstein, A. J.; Lawless, W. N.; Miller, J. S. *Phys. Rev. B: Condens. Matter Mater. Phys.* **1989**, *40*, 11422.
(18) (a) Kopf-Maier, P.; Kopf, H.; Neuse, E. W. *Angew. Chem., Int. Ed. Engl.* **1984**, *23*, 456. (b) Hillard, E.; Vessieres, A.; Thouin, L.; Jaouen, G.; Amatore, C. *Angew. Chem., Int. Ed. Engl.* **2006**, *45*, 285. (c) Popova, L. V.; Babin, V. N.; Belousov, Y. A.; Nekrasov, Y. S.; Snegireva, A. E.; Borodina, N. P.; Shaposhikova, G. M.; Bychenko, O. B.; Raevskii, P. M.; Morozova, N. B.; Liyina, A. I.; Shitkov, K. G. *Appl. Organomet. Chem.* **1993**, *7*, 85. (d) Miklan, Z.; Szabo, R.; Zsoldos-Mady, V.; Remenyi, J.; Banoczi, Z. *Peptide Sci.* **2007**, *88*, 108.
(19) (a) Mealli, C.; Sacconi, L. *Acta Crystallogr.* **1977**, *B33*, 710. (b) Bushnell, G. W.; Dixon, K. R.; Khan, M. A. *Can. J. Chem.* **1978**, *56*, 450.
(20) (a) Clearfield, A.; Singh, P. J.; Bernal, I. *J. Chem. Soc., Chem. Commun.* **1970**, *7*, 389. (b) Epstein, J. M.; Dewan, J. C.; Kepert, D. L.; White, A. H. *J. Chem. Soc., Dalton Trans.* **1974**, 1949. (c) Dewan, J. C.; Kepert, D. L.; White, A. H. *J. Chem. Soc., Dalton Trans.* **1975**, 490. (d) Nakajima, H.; Nagao, H.; Tanaka, K. *J. Chem. Soc., Dalton Trans.* **1996**, 1405.
(21) (a) Koizumi, T.-A.; Tanaka, K. *Inorg. Chim. Acta* **2004**, *357*, 3666. (b) Tsuda, T.; Ohba, S.; Takahashi, M.; Ito, M. *Acta Crystallogr., Sect. C: Cryst. Struct. Commun.* **1989**, *45*, 887. (c) Gatteschi, D.; Mealli, C.; Sacconi, L. *J. Am. Chem. Soc.* **1973**, *95*, 2736. (d) Gatteschi, D.; Mealli, C.; Sacconi, L. *Inorg. Chem.* **1976**, *15*, 2774. (e) Sacconi, L.; Mealli, C.; Gatteschi, D. *Inorg. Chem.* **1974**, *13*, 1985. (f) Griffith, W. P.; Koh, T. Y.; White, A. J. P.; Williams, D. J. *Polyhedron* **1995**, *14*, 2025.
(22) (a) Bandoli, G.; Dolmella, A. *Coord. Chem. Rev.* **2000**, *209*, 161. (b) Dong, G.; Yu-ting, L.; Chun-ying, D.; Hong, M.; Qing-jin, M. *Inorg. Chem.* **2003**, *42*, 2519. (c) Rheingold, A. L.; Mueller-Westerhoff, U. T.; Swiegers, G. F.; Haas, T. J. *Organometallics* **1992**, *11*, 3411.
(23) (a) Pastene, R.; Bozec, H. L.; Moya, S. A. *Inorg. Chem. Commun.* **2000**, *3*, 376. (b) Gelin, F.; Thummel, R. P. *J. Org. Chem.* **1992**, *57*, 3780.

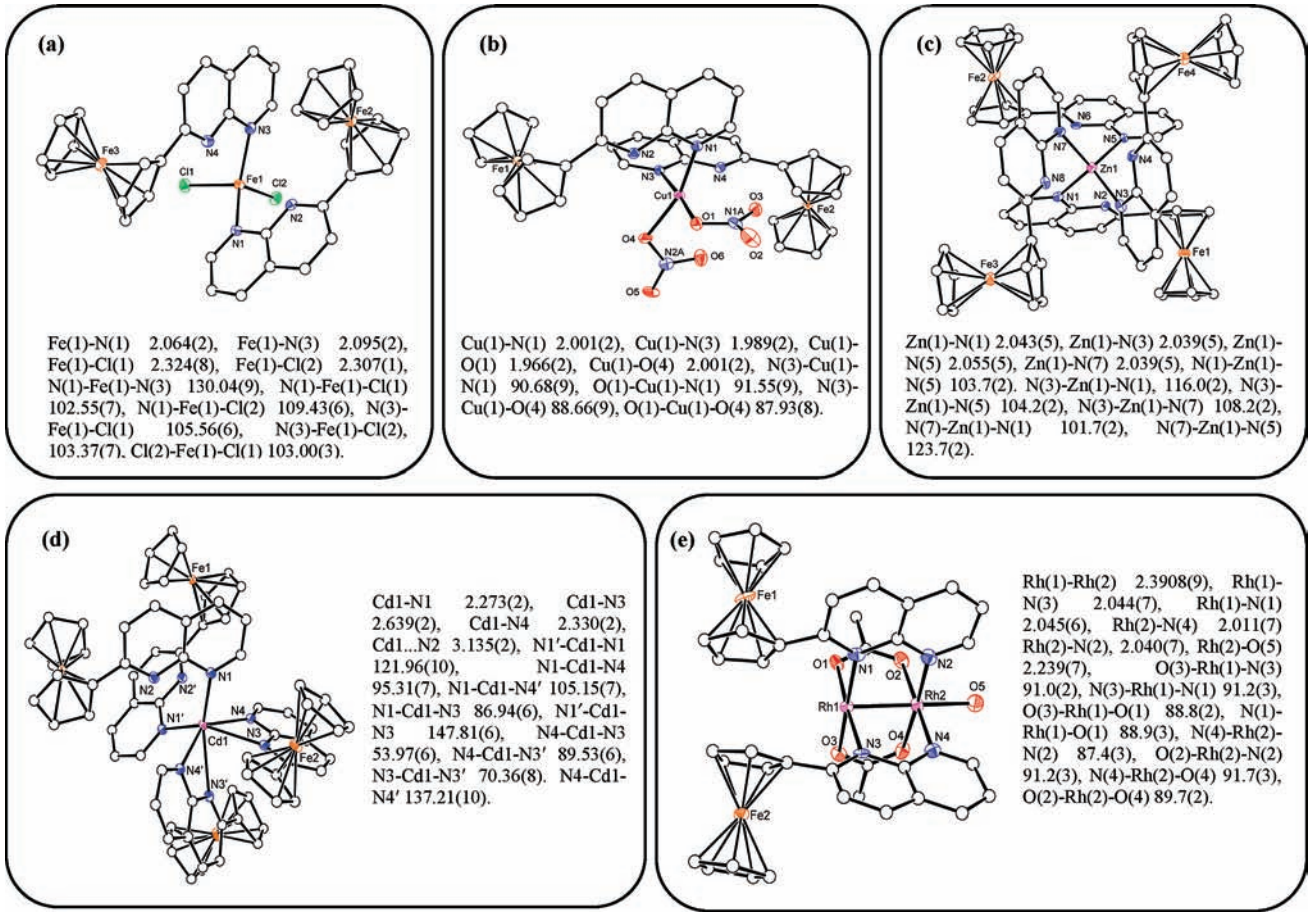

Figure 1. ORTEP diagrams (50% probability thermal ellipsoids) of (a) $[FeCl_2(FcNP)_2]$ (**1**), (b) $[Cu(FcNP)_2(NO_3)_2]$ (**2**), (c) the dicationic $[Zn(FcNP)_4]$ unit in **3**, (d) the dicationic $[Cd(FcNP)_4]$ unit in **4**, and (e) the dicationic $[Rh_2(FcNP)_2(OAc)_2(H_2O)]$ unit in **5**. Carbon atoms are shown as circles of arbitrary radius. Hydrogen atoms are omitted for the sake of clarity. Important bond distances (Å) and angles (deg) are listed with the diagram.

90.68(9)°, whereas other N−Cu−O and O−Cu−O angles vary within a short range of 87.93(8)−91.55(9)°. The ESI-MS spectrum of **2** reveals a peak at *m*/*z* 691, attributed to a $[Cu(FcNP)_2]^+$ species.

The Zn atom in complex **3** forms a tetrahedral complex wrapped with four FcNP ligands. Each ligand is coordinated to the metal ion through the distal N atom. The tetrahedron consists of four Zn−N distances in the range 2.039(5)−2.055(5) Å and N−Zn−N angles in the range of 101.7(2)−123.7(2)° (Figure 1c). The ESI-MS spectrum of **3** exhibits signal at *m*/*z* 661 ($z = 2$), attributed to $[Zn(FcNP)_4]^{2+}$.

Four FcNP ligands coordinate to the Cd atom in complex **4** in a distorted octahedral geometry, unlike the tetrahedral environment of Zn in **3**. Complex $[Cd(FcNP)_4]^{2+}$ has a crystallographically imposed C_2 symmetry and one-half of the molecule is observed in the asymmetric unit. Two cis FcNP ligands occupy four sites through both the proximal and distal nitrogen atoms of NP units in chelate modes. The remaining two sites are coordinated by two FcNP ligands through the distal N atoms (Figure 1d). The Cd−N (κN_8-FcNP) distance is 2.273(2) Å. Short and long Cd−N (κ^2N_1,N_8-FcNP) distances of 2.330(2) and 2.639(2) Å and an acute N3−Cd1−N4 angle of 53.97(6)° are the features for the chelating FcNP ligands. Other acute N−Cd−N angles range from 70.36(8)° to 89.53(6)°, and the obtuse N−Cd−N angles vary in the range 95.31(7)−147.81(6)°, reflecting severe distortions from the ideal octahedral geometry. The NP ligand, devoid of Fc appendage, is reported to form an octa-coordinate complex $[Cd(NP)_4]^{2+}$, in which each NP binds the central Cd atom through both nitrogen atoms in the κ^2N_1,N_8 chelate mode, with Cd−N distances are in the range 2.42(2)−2.73(3) Å.[20b] The ESI-MS spectrum of complex **4** reveals a peak at *m*/*z* 685 ($z = 2$) corresponding to the species $[Cd(FcNP)_4]^{2+}$.

Reaction of preformed metal−metal bonded dirhodium(II) complex $[Rh_2(\mu\text{-}O_2CCH_3)_2(CH_3CN)_6][BF_4]_2$ with FcNP in 1,2-dichloroethane and subsequent crystallization in the presence of $[n\text{-}Bu_4N][OTf]$ provides $[Rh_2(\mu\text{-}FcNP)_2(\mu\text{-}O_2CCH_3)_2(H_2O)][OTf]_2$ (**5**). The molecular structure of **5** consists of a dirhodium core with two cis FcNP ligands, arranged in a head-to-head (HH) fashion bridging metal centers (Figure 1e). The metal−metal bond distance is 2.3908(9) Å, similar to NP-bridged Rh−Rh single-bond distances previously reported.[24] The Rh−N distances are in the range 2.011(7)−2.045(6) Å. The dirhodium unit is

(24) (a) Aguirre, J. D.; Lutterman, D. A.; Angeles-Boza, A. M.; Dunbar, K. R.; Turro, C. *Inorg. Chem.* **2007**, *46*, 7494. (b) Campos-Fernández, C. S.; Thomson, L. M.; Galán-Mascarós, J. R.; Ouyang, X.; Dunbar, K. R. *Inorg. Chem.* **2002**, *41*, 1523. (c) Campos-Fernández, C. S.; Ouyang, X.; Dunbar, K. R. *Inorg. Chem.* **2000**, *39*, 2432. (d) Tikkanen, W. R.; Binamira-Soriaga, E.; Kaska, W. C.; Ford, P. C. *Inorg. Chem.* **1984**, *23*, 141. (e) Tikkanen, W. R.; Binamira-Soriaga, E.; Kaska, W. C.; Ford, P. C. *Inorg. Chem.* **1983**, *22*, 1147.

Scheme 2. Schematic Representation of (a) the Rotational Angle (ϕ_1) and (b) the Inclination Angle (ϕ_2)

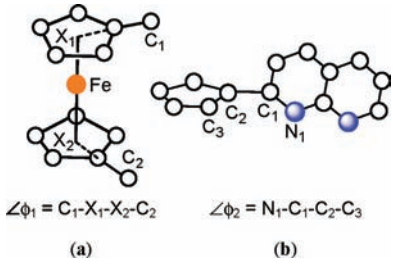

additionally bridged by two acetates, forming a paddlewheel structure, and the Rh−O distances are in the range 2.030(6)−2.060(6) Å. One of the axial sites is occupied by a water molecule with a Rh2−O5 distance of 2.239(7) Å. Approach of a ligand to the other axial site is blocked by two ferrocene appendages. An intramolecular face-to-face $\pi-\pi$ stacking interaction between NP-substituted Cp units of two FcNP ligands is noted with a centroid-to-centroid separation of 3.3195(2) Å (Figure S13, Supporting Information). The ESI-MS signal at *m*/*z* 1039 is attributed to the $[\{Rh_2(FcNP)_2(OAc)_2\}^{2+} + (BF_4^-)]^{1+}$ ion on the basis of the mass and isotopic distribution pattern.

The coordination environment of the metal ions in compounds **1**−**5** deviates considerably from its corresponding ideal geometry. For cases where comparison is possible, the composition and structures of FcNP complexes are different from those of corresponding NP compounds.[19−21] Although 1,8-naphthyridine is widely known to bridge a variety of metal ions, the κN_8 mode of coordination through the distal nitrogen atom of FcNP appears to be most prevalent, present in compounds **1**−**4**. In complex **4**, two FcNP ligands chelate to Cd^{II} in κ^2N_1,N_8 modes as well. The bridging mode of FcNP is noted for a preformed dimetal precursor, as in **5**.[25] A ESI-MS study reveals that the identity of each complex, as revealed in the solid-state structure, is mostly retained in solution.

Metallacycles Based on $FcNP_2$. Introduction of a NP unit to each Cp ring in ferrocene provides metallacycles upon complexation with transition metal ions.[26] A selected set of metrical parameters concerning structural varieties is closely scrutinized. Two torsional angles reflect the conformation of $FcNP_2$ in these structures.[22] The torsional angle ϕ_1, as described in Scheme 2a, is a measure of the rotation of two NP units about the Cp(centroid)−Fe−Cp(centroid) axis, hereinafter referred to as the "rotational angle". The torsional angle ϕ_2 is the measure of the deviation of the NP plane from its associated Cp plane (Scheme 2b), hereinafter referred to as the "inclination angle". Relevant parameters pertaining to the disposition of $FcNP_2$ in complexes **6**−**10** are compared in Table 1.

1:1 Cu^I/Ag^I and $FcNP_2$. In an earlier communication,[26] we reported the structures of discrete rectangular-shaped metallamacrocycles of formula $[M_2(FcNP_2)_2][X]_2$ (M = Cu, X = ClO_4 (**6**); M = Ag, X = OTf (**7**)), obtained by the treatment of Cu^I and Ag^I with $FcNP_2$ in 1:1 ratios. For the sake of comparison and completeness, their structures are depicted in Figure 2. Molecular structures reveal a head-on arrangement of two $FcNP_2$ ligands linked by metal ions. Each copper atom coordinated to distal nitrogen atoms of two $FcNP_2$ in a quasi-linear environment with Cu−N distances of 1.889(3) Å and 1.898(3) Å and an N2−Cu1−N3 angle of 176.47(13)° in **6**. The Ag atom in **7** was found to be disordered over two positions, separated by 0.696 Å with occupancies of 0.62 (Ag1) and 0.38 (Ag1′), located at the pocket created by two NP units from two $FcNP_2$'s, leading to a metallacycle that is smaller in width (Fe···Fe 9.127(1) Å) in comparison to "$[\{Cu(FcNP_2)\}_2]^{2+}$" (Fe···Fe 11.104(3) Å; Figure 2). The rotational angles (ϕ_1) 3.7° and 0.1° for compounds **6** and **7**, respectively, reveal an eclipsed arrangement of the Cp rings. The NP appendages were found to be eclipsed as well. The inclination angles (ϕ_2) for compound **6** are 15.0° and 16.7° and for compound **7** are 13.3° and 20.5° (Table 1).

$PdCl_2$ and $FcNP_2$. $PdCl_2$ forms a neutral chelate complex $[PdCl_2(FcNP_2)]$ (**8**) in which the Pd atom links two NP units of $FcNP_2$ through distal N atoms in trans geometry (Figure 3). The geometry at Pd in **8** is square planar, with cis angles of 88.52(6)° and 91.53(6)°. The Pd−N and Pd−Cl distances are 2.020(2) Å and 2.315(1) Å, respectively. The plane constructed by the Pd and the coordinating atoms (within 0.067 Å) is near orthogonal to the NP planes, the interplanar angle being 78.459°. The NP rings rotate away considerably to form a chelate complex with Pd, as revealed in the rotational angle (ϕ_1) value of 88.2°. Interestingly, the inclination angle (ϕ_2) is 17.5°, similar to that observed for the "head-on" dimers **6** and **7**.

2:1 Cu^I and $FcNP_2$. The reaction of 2 equiv of Cu^I with $FcNP_2$ results in $[Cu_2(FcNP_2)(OClO_3)][ClO_4]$ (**9**) in quantitative yield, the structure of which is established from an X-ray diffraction study. The NP appendages in $FcNP_2$ bridge two copper atoms in trans geometry, as shown in Figure 4. The coordination geometry for two metals can be described as linear two-coordinate: one is bonded to proximal nitrogen atoms, and the second one is bonded to distal nitrogen atoms of NP units. The inner copper makes an N4−Cu2−N2 angle of 178.01(15)° with shorter Cu−N distances (Cu2−N4 1.875(4) Å, Cu2−N2 1.879(3) Å). In contrast, the geometry of the outer copper deviates considerably from linearity, as reflected in the N1−Cu1−N3 angle (168.68(16)°), involving longer Cu−N distances (Cu1−N1 1.943(4) Å and Cu1−N3 1.946(4) Å). One of the perchlorate anions is located in the vicinity of Cu1. The oxygen atom nearest to Cu1 was found to be disordered over two positions with occupancies of 0.85 (O1) and 0.15 (O8). The Cu1···O1 and Cu1···O8 distances are 2.382(4) Å and 2.285(2) Å, respectively (see Figure S8, Supporting Information). It should be further noted that remaining oxygen atoms were also severely disordered and were modeled satisfactorily. The NP units and dicopper core reside on a plane with a maximum deviation from the mean plane of 0.28 Å.

(25) (a) Majumdar, M.; Patra, K. S.; Kanan, M.; Dunbar, K. R.; Bera, J. K. *Inorg, Chem.* **2008**, *47*, 2212. (b) Patra, S. K.; Sadhukhan, N.; Bera, J. K. *Inorg, Chem.* **2006**, *45*, 4007. (c) Bera, J. K.; Schelter, E. J.; Patra, S. K.; Bacsa, J.; Dunbar, K. R. *Dalton Trans.* **2006**, 4011.

(26) Sadhukhan, N.; Patra, S. K.; Sana, K.; Bera, J. K. *Organometallics* **2006**, *25*, 2914.

Table 1. The Conformations of Cp Rings, Rotational Angle (deg), Inclination Angle (deg), and Bent Angle (deg) for $FcNP_2$ and Compounds **6**−**10**

Compound	Disposition of $FcNP_2$	Conformation	Rotational Angle (ϕ_1)	Inclination Angle (ϕ_2)	Bent Angle[a] ($\angle X_1$-Fe-X_2)
$FcNP_2$		Antiperiplanar staggered	180	13.8	180.0
6		Synperiplanar eclipsed	3.7	15.0 16.7	177.2
7		Synperiplanar eclipsed	0.1	20.5 13.3	176.0
8		Synclinal staggered	88.2	17.5	179.2
9		Synclinal eclipsed	80.2	29.5 38.0	174.1
10		Synperiplanar eclipsed	2.4	11.6 11.7	178.3

[a] X_1 and X_2 are centroids of the Cp rings (see Scheme 2).

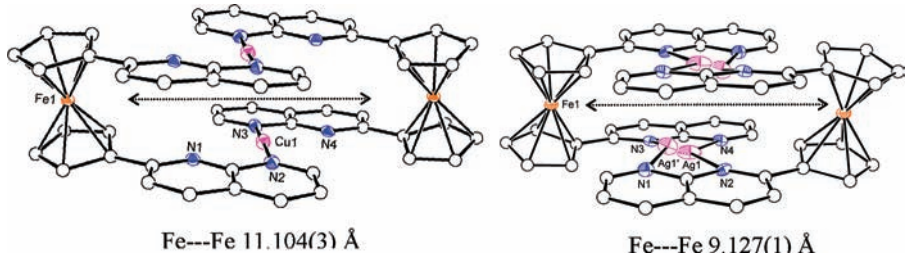

Figure 2. ORTEP diagram (50% probability thermal ellipsoids) of the dicationic unit $[\{Cu(FcNP_2)\}_2]^{2+}$ in **6** and $[\{Ag(FcNP_2)\}_2]^{2+}$ in **7** with important atoms labeled. Carbon atoms are shown as circles of arbitrary radius. Hydrogen atoms are omitted for the sake of clarity.

The μ-κ^2N_1,N_8:κ^2N_1',N_8' coordination of $FcNP_2$ forces two copper atoms to acquire a Cu···Cu distance of 2.466(1) Å, which is significantly shorter than the corresponding distances 2.506(2)[27] and 2.533(2) Å reported[28] for the dicopper(I) complex bridged by two independent naphthyridine ligands. It is intriguing that the anchoring of NPs to ferrocene results in a shorter metal···metal distance (Scheme 3). The short Cu···Cu separation in **9** is primarily attributed to ligand architecture, although the presence of metallophilic interactions has been supported and refuted as well for similar dicopper(I) complexes.[29,31]

The structural resemblance between **8** and **9** merits close inspection. It appears that a rotational angle ϕ_1 close to 90° is the prerequisite for a chelate complex. The rotational angle (ϕ_1) of 80.2° noted for **9** is smaller than that observed in **8** by 8°, presumably caused by the larger radius of Pd^{II} compared to Cu^{I}. Inclination angles (ϕ_2) of 29.48° and 37.96° are the largest (Table 1) in **9**, resulting from the bidentate bridging mode of each NP unit. The overall strain in the

(27) Munakata, M.; Maekawa, M.; Kitagawa, S.; Adachi, M. *Inorg. Chim. Acta* **1990**, *167*, 181.
(28) Maekawa, M.; Munakata, M.; Kitagawa, S.; Kuroda-sowa, T.; Suenaga, Y.; Yamamoto, M. *Inorg. Chim. Acta* **1998**, *271*, 129.
(29) (a) Che, C.-M.; Mao, Z.; Miskowski, V. M.; Tse, M.-C.; Chan, C.-K.; Cheung, K.-K.; Phillips, D. L.; Leung, K.-H. *Angew. Chem., Int. Ed. Engl.* **2000**, *39*, 4084. (b) Pyykkö, P. *Chem. Rev.* **1997**, *97*, 597. (c) Poblet, J.-M.; Benard, M. *Chem. Commun.* **1998**, 1179. (d) Pyykkö, P.; Mendizabal, F. *Inorg. Chem.* **1998**, *37*, 3018.
(30) (a) Budzikiewicz, H.; Djerassi, C.; Williams, D. H. *Interpretation of Mass Spectra of Organic Compounds*; Holden-Day, Inc.: San Fransisco, CA, 1964. (b) Silverstein, R. M. *Spectrocopic Identification of Organic Compounds*, 5th ed.; John Wiley & Sons, Inc.: New York, 1991.
(31) (a) Siemeling, U.; Vorfeld, U.; Neumann, B.; Stammler, H.-G. *Chem. Commun.* **1997**, 1723. (b) Neumann, B.; Siemeling, U.; Stammler, H.-G.; Vorfeld, U.; Delis, J. G. P.; van Leeuwen, P. W. N. M.; Vrieze, K.; Fraanje, J.; Goubitz, K.; de Biani, F. F.; Zanello, P. *J. Chem. Soc., Dalton Trans.* **1997**, 4705.

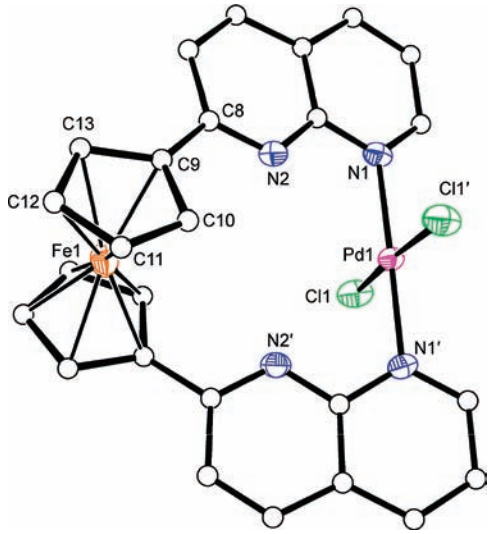

Figure 3. ORTEP diagram (50% probability thermal ellipsoids) of $[PdCl_2(FcNP_2)]$ (**8**) with important atoms labeled. Carbon atoms are shown as circles of arbitrary radius. Hydrogen atoms are omitted for the sake of clarity. Selected bond distances (Å) and angles (deg): Pd1−N1 2.020(2), Pd1−Cl1 2.315(1), N1−Pd1−Cl1 88.52(6), N1′−Pd1−N1 178.87(10), N1′−Pd1−Cl1′ 88.52(6), N1′−Pd1−Cl1′ 88.52(6), N1−Pd1−Cl1′ 91.53(6), N1′−Pd1−Cl1 91.53(6), Cl1′−Pd1−Cl1 175.09(3). Symmetry code: $-x + 1, y, -z + 1.5$.

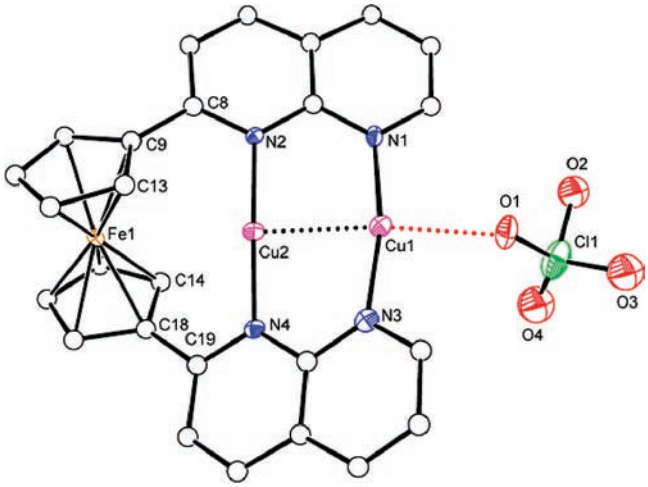

Figure 4. ORTEP diagram (50% probability thermal ellipsoids) of $\{Cu_2(FcNP_2)(OClO_3)\}^+$ in **9** with important atoms labeled. Carbon atoms are shown as circles of arbitrary radius. Selected bond distances (Å) and angles (deg): Cu(2)−Cu(1) 2.4662(8), Cu(2)−N(4) 1.875(4), Cu(2)−N(2) 1.879(3), Cu(1)−N(1) 1.943(4), Cu(1)−N(3) 1.946(4), Cu(1)−O(1) 2.382(4), N(4)−Cu(2)−N(2) 178.01(15), N(4)−Cu(2)−Cu(1) 90.14(11), N(2)−Cu(2)−Cu(1) 88.87(11), N(1)−Cu(1)−N(3) 168.68(16), N(1)−Cu(1)−Cu(2) 85.24(11), N(3)−Cu(1)−Cu(2) 83.44(12), C(13)−C(9)−C(8)−N(2) 29.48, C(14)−C(18)−C(19)−N(4) 37.96.

structure of **9** is manifested in the bent angle, described by a Cp(centroid)−Fe−Cp(centroid) angle of 6° away from linearity.

$ZnCl_2$ and $FcNP_2$. We reported earlier a tetrameric compound $[ZnCl_2(FcNP_2)]_4$ (**10**) obtained from the reaction of $FcNP_2$ and $ZnCl_2$.[26] Each discrete unit of $[ZnCl_2(FcNP_2)]_4$ consists of alternating $ZnCl_2$ and $FcNP_2$ units (Figure 5a). The overall structure of metallamacrocycle **10** consists of a Zn_4 square of dimensions 9.584(2) Å spanned by $FcNP_2$ units. The Fc units are alternatively above and below the plane of the Zn_4 square, forming a Fe_4 tetrahedron consisting of four isosceles triangles with Fe···Fe distances of 9.271(3) and 7.844(2) Å. Each Fe atom is connected to two neighboring Zn's by Cp−NP units with Fe···Zn distances of 5.995(2) and 6.261(2) Å (Figure 5b). The coordination geometry of Zn^{II} resembles closely that of the central Fe^{II} in $FeCl_2(FcNP)_2$ (**1**). A single NP appendage in the Cp ring of FcNP provides discrete monomer product **1**, whereas two NP units appended to two Cp rings of $FcNP_2$ result in self-assembled cyclic structure **10**.

Scheme 3. $FcNP_2$ and NP Bridged Di-Copper(I) Units and the Corresponding Cu···Cu Distances

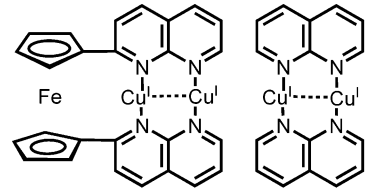

Cu^I---Cu^I	2.466(1) Å[a]	2.506(2) Å[27]
		2.533(2) Å[28]

[a] This work.

Interconversion between 6 and 9. The metal-to-ligand ratio is different in compounds **6** and **9**. A 1:1 mixture of Cu^I and $FcNP_2$ provides the "head-on" dimer **6**, whereas the "bridged-chelate" dimer **9** results from a metal-to-ligand ratio of 2:1. It was possible to convert **6** to **9** by introducing a requisite amount of Cu^I. The addition of 2 equiv of Cu^I to a nitromethane solution of **6** resulted in a dark-red solid that was characterized as **9**. The reverse reaction, that is the reaction of **9** with 1 equiv of $FcNP_2$ in nitromethane, led to **6**. Both compounds were obtained in high yields via interconversion routes and were characterized by matching the elemental analyses, the mass spectral data (vide infra), and the unit cell parameters with the authentic compounds.

Mass Spectra. Examination of the mass spectra of compounds **6**−**9** provides insight into their structures in solution. The ESI-MS of **6** in a 9:1 acetonitrile/nitromethane solution reveal ions at mass-to-charge (*m*/*z*) ratios of 1109 and 1145, attributed to $[\{M\}^{2+} + ClO_4^-]^+$ and $[\{M\}^{2+} + ClO_4^- + 2H_2O]^+$, respectively, where $\{M\}^{2+}$ is $[Cu_2(FcNP_2)_2]^{2+}$, followed by an ion signal at a mass-to-charge (*m*/*z*) ratio of 1159. The signal at *m*/*z* 1159 is assigned as $[\{M\}^{2+} + H_2O + NO + ClO_4^-]^+$ on the basis of simulated mass and isotopic distribution patterns. The calculated and recorded mass distributions are compared in Figure 6. The source of nitrosyl (NO) is the solvent nitromethane. Organic nitro compounds are known to produce NO through the intermediacy of the NO_2 radical under the experimental conditions used for mass spectroscopy.[30] The intensity ratio of 1:3 for signals at *m*/*z* 1109 and 1145 remains invariant; however, the intensity of the signal at *m*/*z* 1159 was found to vary in different runs. Interestingly, the NO-incorporated product was identified only for compound **6**.

It is rather remarkable that the integrity of the dimer **6** is retained in appreciable amounts under the ESI-MS conditions. However, the most intense signal at *m*/*z* 505, attributed to $\{Cu(FcNP_2)\}^{1+}$, dominates the mass spectrum of **6**.

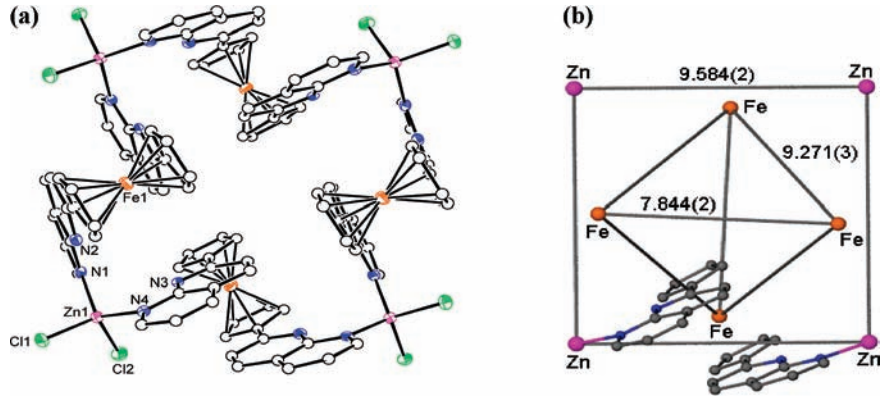

Figure 5. ORTEP diagram (50% probability thermal ellipsoids) of (a) $[ZnCl_2(FcNP_2)]_4$ (**10**) and (b) the skeletal arrangement of Zn_4Fe_4 moiety with illustration of the Cp−NP unit spanning the Fe and Zn atoms.

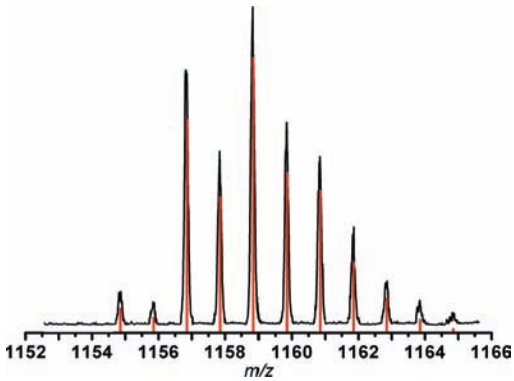

Figure 6. Simulated (red line) and experimental mass distributions (black line) for ion $[\{M\}^{2+} + H_2O + NO + ClO_4^-]^+$ where $\{M\}^{2+}$ is $[Cu_2(FcNP_2)_2]^{2+}$.

Although the monomer is present predominantly in solution, crystallization results in the dimeric product in near-quantitative yield.

The signal at *m*/*z* 1249, assigned for $[\{Ag_2(FcNP_2)_2\}^{2+} + OTf^-]^+$, along with the most intense signal at *m*/*z* 549, corresponding to $[Ag(FcNP_2)]^{1+}$, were observed in the mass spectrum of **7**. The ESI-MS data of **8** reveal a signal at *m*/*z* 583 which is assigned to $[M - Cl]^+$ $\{M = PdCl_2(FcNP_2)\}$ confirming 1:1 metal-to-ligand composition in solution.

The ESI-MS data of **9** exhibit a signal at *m*/*z* 669 which is attributed to $[\{M\}^{2+} + ClO_4^-]^+$, where $\{M\}$ is $[Cu_2(FcNP_2)]$. The most intense signal at *m*/*z* 505 is assigned to the 1:1 complex $[Cu(FcNP_2)]^+$, a species which was also observed in the mass spectrum of **6**.

The most notable feature of this work is the isolation of two topologically different structures obtained by employing Cu^I and $FcNP_2$ in different ratios. The "head-on" dimer is obtained from 1:1 metal-to-ligand assembly, and the "bridged-chelate" complex is the isolated product when a metal-to-ligand ratio of 2:1 is employed. Both complexes were identified in their corresponding mass spectrum along with a ubiquitous signal at *m*/*z* 505, attributed to $[Cu(FcNP_2)]^+$. It is our assertion that compound **6** exists in equilibrium with the monomeric 1:1 species $[Cu(FcNP_2]^+$, for which a "chelate" structure, depicted in Scheme 4a, is proposed. Precedence for a similar structure, $[Cu(Fc*Py_2]^+$ ($Fc*Py_2$ = 1,1′-bis(2-pyridyl)octamethylferrocene), exists in the literature (Scheme 4b).[31] Further support for a chelate compound

Scheme 4. Structures of (a) $[Cu(FcNP_2)]^+$ (this work), (b) $[Cu(Fc*Py_2)]^+$,[31] and (c) $[Cu(FcQu_2)]^+$ [32]

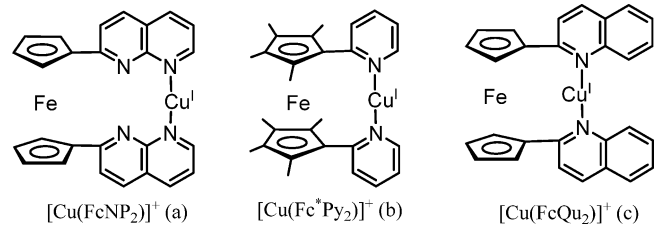

stems from the structure of $[Cu(FcQu_2)]^+$ ($FcQu_2$ = 1,1′-bis(quinolin-2-yl)ferrocene) (Scheme 4c), which we have carried out in our laboratory recently.[32]

The addition of 2 equiv of $[Cu(CH_3CN)_4][ClO_4]$ to an acetonitrile/nitromethane solution of **6** and the recording of the mass spectrum revealed a mixture of the "head-on" dimer (*m*/*z* 1109), "chelate" monomer (*m*/*z* 505), and "bridged-chelate" dimer (*m*/*z* 669) compounds (Scheme 5). The ratio of the "head-on" dimer **6** and "bridged-chelate" dimer **9** was found to be 1:1, even when the reaction was allowed for a prolonged period. In contrast, the "bridged-chelate" complex **9** converts fully to **6** on treatment with $FcNP_2$. The parent signal at *m*/*z* 669 for the "bridged-chelate" dimer vanishes, and a new signal at *m*/*z* 1159 for the "head-on" dimer appears. It is concluded from ESI-MS experiments that both 1:1 and 2:1 Cu^I−$FcNP_2$ complexes exist predominantly as the monomer $[Cu(FcNP_2]^+$ in solution. The equilibrium is shifted toward the "bridged-chelate" dimer on addition of Cu^I to the 1:1 complex, whereas the 2:1 dimer transforms to the 1:1 complex completely on addition of $FcNP_2$ (Scheme 5). The "head-on" or the "bridged-chelate" dimer is the isolated product in the solid state depending on the metal-to-ligand ratio. Despite the chelate complex $[Cu(FcNP_2]^+$ being the major species in solution, we have been unsuccessful in isolating it in our study, and either **6** or **9** was obtained in quantitative amount by crystallization.

Electrochemistry. The electrochemical behavior of FcNP, $FcNP_2$, and compounds **1**−**9** was investigated by cyclic voltammetric studies in propylene carbonate, and the redox potential values are given in Table 2. The FcNP exhibits

(32) Bera, J. K. Unpublished work. Cell parameters of $[Cu(FcQu_2)][ClO_4]$: *a* (Å) = 7.2624(13), *b* (Å) = 10.5112(19), *c* (Å) = 16.5818(3), α (deg) = 77.865(3), β (deg) = 87.88(3), γ (deg) = 72.277(3), *V* (Å^3) = 1178.28(4).

Scheme 5. Interconversion Reactions among Metallamacrocycles and the Corresponding ESI-MS Spectrum

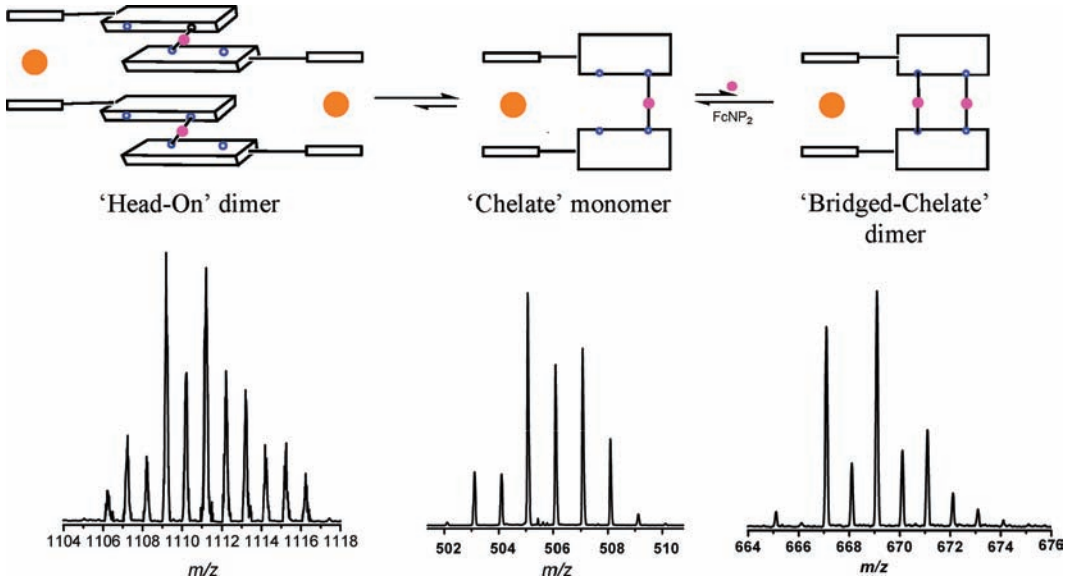

Table 2. Electrochemical Potentials (in volts) from Cyclic Voltammetry for FcNP, $FcNP_2$, and Complexes **1**−**7** and **9** in Propylene Carbonate

compounds	Fc center	metal center	NP center
FcNP	0.53(180)[a]		−1.93[b]
1	0.55(80)[a]	0.083(83)[a]	−1.78[b]
2	0.58(120)[a]		−1.31,[b] −1.92[b]
3	0.58(100)[a]		−1.26,[b] −1.87[b]
4	0.58(130)[a]		−1.33,[b] −1.93[b]
5[c]	0.65(60),[a] 0.77(60)[a]	−0.66(60)[a]	−1.91[b]
$FcNP_2$	0.66(100)[a]		−1.87[b]
6	0.80 (150)[a]	0.33[d]	−1.83[b]
7	0.70 (70)[a]	−0.63[b]	−1.88[b]
9	0.79[d]		−1.03,[b] −1.84[b]

[a] Half-wave potentials evaluated from cyclic voltammetry as $E_{1/2} = (E_{p,a} + E_{p,c})/2$, peak potential differences in mV in parentheses. [b] Peak potentials, $E_{p,c}$, for irreversible processes. [c] Ill-defined reduction waves are observed in the range −1.01 to −1.17 V. [d] Peak potentials, $E_{p,a}$ for irreversible processes.

ferrocene (Fc)-based quasi-reversible oxidation at $E_{1/2} = 0.53$ V and NP-based irreversible reduction at $E_{p,c} = -1.93$ V. A large separation of 180 mV between forward and backward oxidation waves was measured. FcNP-based compounds **1**−**4** show Fc^+/Fc-based reversible oxidations ($E_{1/2}$) in the short range of 0.55−0.58 V. An additional reversible oxidation is recorded for **1** at $E_{1/2} = 0.083(83)$ V corresponding to the central Fe^{III}/Fe^{II} couple. The oxidation processes for complex **1** is shown in Figure 7. NP-centered reduction occurs at $E_{p,c}$ −1.78 V for **1**. Compounds **2**, **3**, and **4** exhibit two irreversible reduction waves at $E_{p,c}$ values of −1.31 and −1.92, −1.26 and −1.87, and −1.33 and −1.93 V, respectively. Compound **5** exhibits two closely spaced reversible oxidations at $E_{1/2} = 0.65(70)$ and 0.77(70) V, indicating weak electronic communication between FcNP ligands through the dirhodium single bond. A reversible reduction wave corresponding to the $[Rh_2]^{4+}/[Rh_2]^{3+}$ couple occurs at $E_{1/2} = -0.66(60)$ V. NP-based irreversible reductions are observed at an $E_{p,c}$ of −1.91 V, including a number of ill-defined irreversible features in the range −1.01 to −1.17 V.

Introduction of the second NP ring in FcNP causes a significant shift (130 mV) for ferrocene-based oxidation toward more positive potential. A reversible oxidation at $E_{1/2} = 0.66(100)$ and an irreversible NP-based reduction occur at $E_{p,c} = -1.87$ V with an associated return wave at $E_{p,a} = 0.52$ V for $FcNP_2$. Ferrocene-based reversible oxidation for compound **6** is observed at $E_{1/2} = 0.80$ V, and the separation of the anodic oxidation peak and the cathodic counter peak is 150 mV. An additional Cu^I/Cu^{II} oxidation appears at $E_{p,a} = +0.33$ V. The NP-based irreversible reduction potential $E_{p,c}$ is observed at −1.83 V. Compound **7** shows similar electrochemical behavior with ferrocene-based reversible oxidation at 0.70(70) V and NP-based reduction at −1.88 V. The irreversible reduction at −0.63 V is attributed to the Ag^+/Ag couple. The cyclic voltammetry of compound **9** is surprisingly featureless, exhibiting a very weak irreversible oxidation wave at $E_{p,a} = 0.79$ V and reduction waves $E_{p,c} = -1.03$ and −1.84 V at the glassy carbon electrode. The low solubility of compounds **8** and **10** did not allow us to carry out electrochemical studies.

Crystal Packing and Noncovalent Interactions. Careful examinations of crystal structures of the compounds reveal interesting features. Stacking interactions between two NP rings, two Cp rings, and Cp···NP rings are observed. The offset-antiparallel stacking between two interacting NP rings, where two hydrogen atoms of one ring lie on top of the nitrogen atoms of another parallelly placed ring (Scheme 6a),

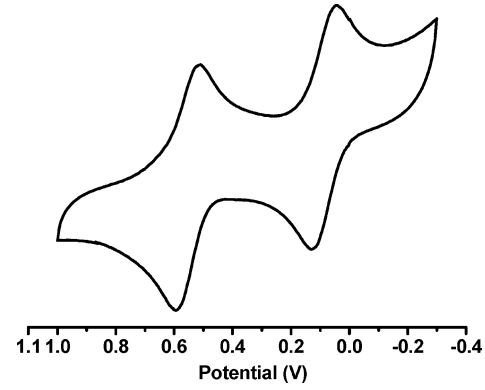

Figure 7. Cyclic voltammogram of **1** measured at a scan rate of 100 mV/s in propylene carbonate.

Scheme 6. (a) NP···NP Stacking Interaction and (b) the Representation of Displacement Angle (α)

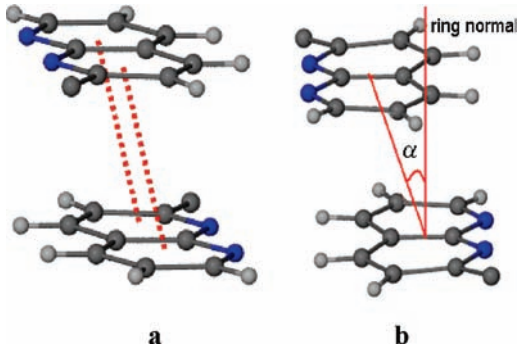

was noticed in FcNP and in compounds **8** and **9**. In the crystal structure of FcNP, NP···NP interactions are localized between two neighboring ligands (Figure 8a), whereas staircase assembly of the molecules is observed in the crystal structure of **8** (Figure S16, Supporting Information). For compound **9**, similar 1-D stacking was observed, which also includes Cp···NP interactions (Figure 8b). The centroid (NP) to centroid (NP) distances are in the range 3.505(1)−3.599(1) Å, and the displacement angles (α), measured as the angle between the ring normal and the centroid vector (Scheme 6b), range from 16.77° to 22.37°. In the case of two pyridine rings, the displacement angles lie from 16° to 40°, and centroid-to-centroid distances are from 3.4 to 4.6 Å, with a higher number of examples found at around 3.8 Å.[33]

Intramolecular face-to-face alignment of Cp rings from two different FcNP's is noted for **5** in which the Cp rings are perfectly eclipsed (Scheme 7a). Intermolecular stacking of Cp units exists in **6**, where the orientation of the Cp rings is staggered (Scheme 7b). The centroid-to-centroid distances in **5** and **6** are 3.320 and 3.425Å, respectively. A crystal packing diagram depicting the Cp···Cp interactions in **5** is provided in Figure S13 (Supporting Information), and the corresponding diagram for **6** is shown in Figure 8c (in green).

The most prominent interaction between the Cp and NP rings is shown in Scheme 8a. This particular type of interaction is noted in the crystal structures of $FcNP_2$, **1**, **3**, and **9**. Representative crystal structures of $FcNP_2$ and **9**, with an illustration of Cp···NP interactions, are shown in Figures S15 (Supporting Information) and 8b (in red), respectively. The distances between the NP ring plane and Cp centroid are 3.457 ($FcNP_2$), 3.260 (**1**), 3.319 (**3**), and 3.476 (**9**). Two other types of Cp···NP interactions, shown in Scheme 8b and c, were observed in compounds **6** and **10**, respectively. Figure 8c and d illustrate the Cp···NP interactions (in red) in the crystal packing diagrams of **6** and **10** having interplanar distances of 3.169 and 3.524 Å, respectively.

The C−H···π interactions dominate crystal structures of **1**, **3**, and **4**. The C−H(NP)···Cp interactions are observed in compounds **1** and **3**, whereas C−H(Cp)···Cp interactions are present in compound **4** (see Figure S17, Supporting Information). The C−H···O interactions between O atoms of the coordinated nitrates and Cp/NP hydrogens are observed in compound **2**, as shown in Figure S18 (Supporting Information).

Concluding Remarks

Mixed-metal compounds incorporating two or four FcNP ligands coordinated to different transition metal ions have been synthesized. A comparison of FcNP-based compounds with corresponding NP analogues reveals that they are different with respect to compositions and structures. Diverse bonding modes of the NP unit ranging from monodentate, bidentate chelating, and binuclear bridging are observed in FcNP compounds. Metallamacrocycles are obtained by the reaction of $CuClO_4$, AgOTf, $PdCl_2(PhCN)_2$, and $ZnCl_2$ with $FcNP_2$. Structural characterization of the isolated compounds suggests that the conformational flexibility of the ferrocenyl rings, the disposition of N atoms in naphthyridine, and the identity of the metal ion dictate the topology of the product. Further, variation in the metal-to-ligand ratio provides compounds with different topologies. A 1:1 Cu^I to $FcNP_2$ assembly results in the "head-on" dimer, and a 2:1 metal-to-ligand assembly yields the "bridged-chelate" dimer. ESI-MS experiments provide insight into their structures in solution.

Experimental Section

General Procedures and Materials. All reactions were carried out under an inert dinitrogen atmosphere with the use of standard Schlenk-line techniques. Solvents were dried by conventional methods, distilled over nitrogen, and deoxygenated prior to use. The metal precursor $Cu(NO_3)_2 \cdot 3H_2O$, $CoCl_2 \cdot 6H_2O$, and $ZnCl_2$ were purchased from SD Fine-Chem Limited, India. $RhCl_3 \cdot xH_2O$ (40% Rh) was purchased from Arora Matthey, Kolkata, and [*n*-Bu_4N][OTf] was purchased from Aldrich. The compounds $[Rh_2(O_2CMe)_2(CH_3CN)_6][BF_4]_2$,[34] $[Cu(CH_3CN)_4][ClO_4]$,[35] $PdCl_2(C_6H_5CN)_2$,[36] $Ag(O_3SCF_3)$,[37] $Cd(BF_4)_2$,[37] and $Zn(O_3SCF_3)_2$[37] were synthesized following literature procedures. FcNP and $FcNP_2$ were prepared by following literature procedures.[23]

Physical Measurements. Elemental analyses were carried out using a Thermoquest CE instruments model EA/110 CHNS-O elemental analyzer. ESI-MS spectra were recorded on a Waters Micromass Quattro Micro triple−quadrupole mass spectrometer. ESI-MS spectra of FcNP, $FcNP_2$, and compounds **1**−**5** were recorded in acetonitrile, whereas a 9:1 acetonitrile−nitromethane mixture was used for compounds **6**, **7**, and **9** and a 1:1 acetonitrile−methanol mixture was used for **8**. The ^{1}H NMR spectrum was obtained on a JEOL JNM-LA 400 MHz spectrophotometer. Infrared spectra were recorded on a Bruker Vertex 70 FTIR spectrophotometer in the ranges from 400 to 4000 cm^{-1} using KBr pellets. Electronic absorptions were measured on a Perkin-Elmer Lambda-20 UV−vis spectrophotometer. Cyclic voltammetric studies were performed on a BAS Epsilon electrochemical workstation

(33) (a) Jainak, C. *J. Chem. Soc., Dalton Trans.* **2000**, 3885. (b) Mishra, B. K.; Sathyamurthy, N. *J. Phys. Chem. Lett. A* **2005**, *109*, 6. (c) Mishra, B. K.; Sathyamurthy, N. *J. Theory Comput. Chem.* **2006**, *5*, 609. (d) Hobza, P.; Selzle, H. L.; Schlag, E. W. *Chem. Rev.* **1994**, *94*, 1767. (e) Tsuzuki, S.; Honda, K.; Uchimaru, T.; Mikami, M.; Tanabe, K. *J. Am. Chem. Soc.* **2002**, *124*, 124. (f) Hunter, C. A. *Chem. Soc. Rev.* **1994**, 101.

(34) Pimblett, G.; Garner, C. D.; Clegg, W. *J. Chem. Soc., Dalton Trans.* **1986**, 1257.
(35) Kubas, G. J. *Inorg. Synth.* **1979**, *19*, 90.
(36) Doyle, J. R.; Slade, P. E.; Jonassen, H. B. *Inorg. Synth.* **1960**, *6*, 218.
(37) Dixon, N. E.; Jackson, W. G.; Lawrance, G. A.; Sargeson, A. M. *Inorg. Synth.* **1983**, *22*, 103.

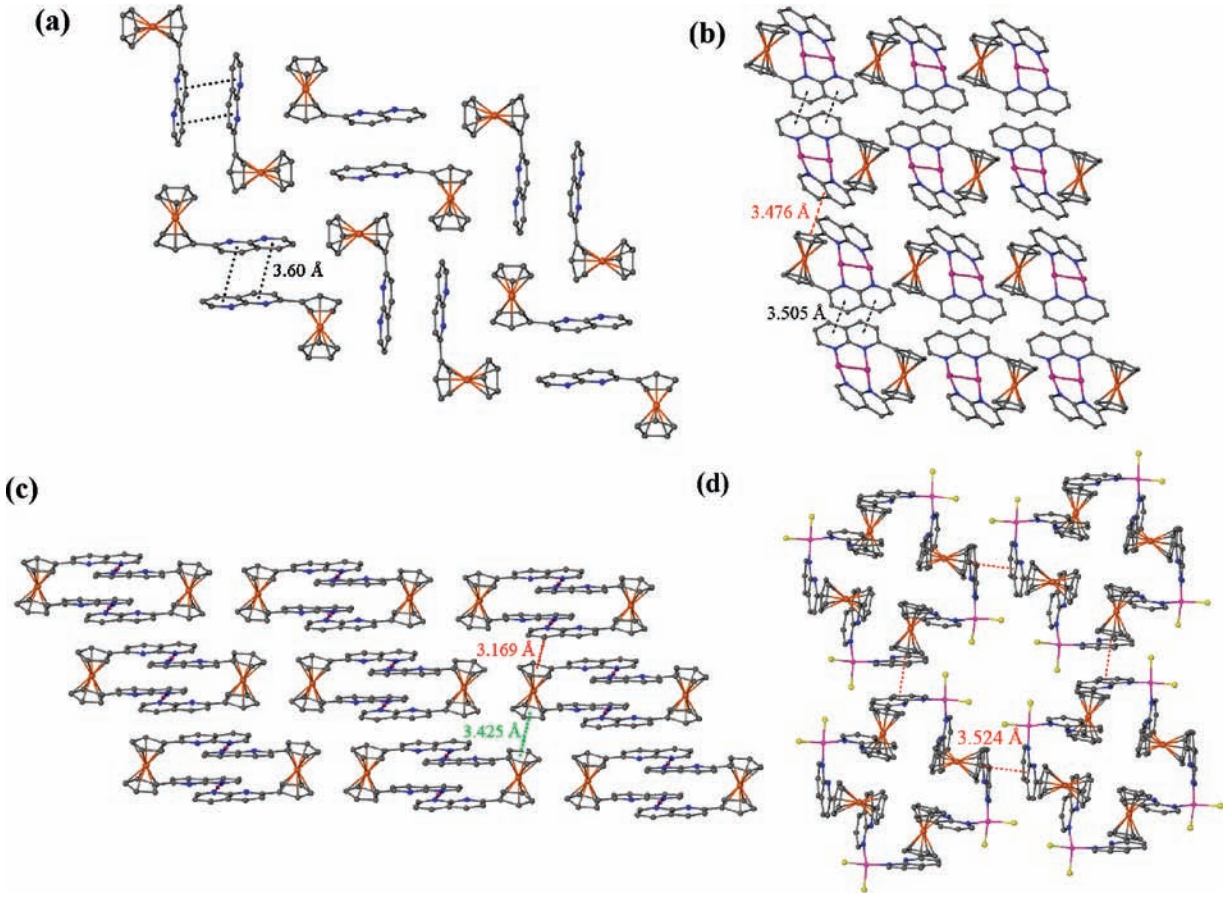

Figure 8. Packing diagrams of compounds (a) FcNP, (b) **9**, (c) **6**, and (d) **10**. The NP···NP, Cp···Cp, and Cp···NP interactions are shown in black, green, and red dotted lines, respectively.

Scheme 7. Face-to-Face Cp···Cp Interactions (a) in Eclipsed and (b) in Staggered Orientations

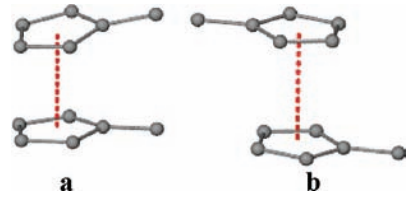

Scheme 8. Different Types of Cp···NP Interactions

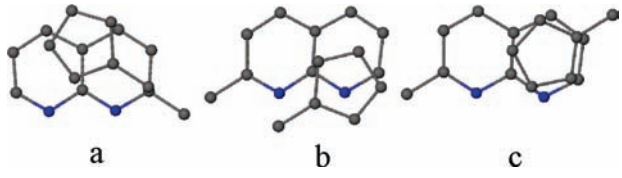

in acetonitrile with 0.1 M tetra-*n*-butylammonium hexafluorophosphate ($TBAPF_6$) as the supporting electrolyte. The working electrode was a BAS Pt disk electrode. The reference electrode was Ag/AgCl, and the auxiliary electrode was a Pt wire. The ferrocene/ferrocenium couple occurs at $E_{1/2} = +0.51$ (70) V versus Ag/AgCl under the same experimental conditions. The potentials are reported in volts; the ΔE ($E_{p,a} - E_{p,c}$) values are in millivolts at a scan rate of 100 mV s^{-1}.

Syntheses. [$FeCl_2$(FcNP)$_2$] (1). FcNP (52 mg, 0.166 mmol) was added to an acetonitrile solution (15 mL) of $FeCl_2$ (10 mg, 0.079 mmol), and the mixture was stirred for 8 h at room temperature. The resulting red solution was concentrated under a vacuum, and 15 mL of diethyl ether was added with stirring to induce precipitation. The red solid residue was filtered, washed with diethyl ether (2 × 15 mL), and dried under a vacuum to give **1**. Yield: 52 mg (87%). X-ray-quality crystals were grown by layering petroleum ether onto a saturated dichloromethane solution of **1** inside an 8 mm o.d. vacuum-sealed glass tube. Anal. calcd for $C_{36}H_{28}N_4Cl_2Fe_3$: C, 57.26; H, 3.74; N, 7.42. Found: C, 57.11; H, 3.67; N, 7.40. ESI-MS: *m*/*z* 719 [M − Cl]$^+$. IR (KBr, cm^{-1}): ν (FcNP) 1612 (vs), 1572(s), 1530 (s), 1503 (s), 1440 (m), 1409 (m), 1383 (s), 1151 (m), 839 (m), 498 (m). UV−vis (CH_3CN, λ_{max}, nm (log ε)): 254 (4.96), 312 (4.93), 3.58 (4.83), 575 (3.75).

[Cu(FcNP)$_2$(NO$_3$)$_2$] (2). The reaction of $Cu(NO_3)_2 \cdot 3H_2O$ (12 mg, 0.05 mmol) and FcNP (33 mg, 0.105 mmol) was carried out following a procedure similar to that described for the synthesis of complex **1**. Yield: 35 mg (86%). X-ray-quality crystals were grown by layering petroleum ether onto a saturated dichloromethane solution of complex **2** inside an 8 mm o.d. vacuum-sealed glass tube. Anal. calcd for $C_{36}H_{28}N_6O_6Fe_2Cu_1$: C, 53; H, 3.46; N, 10.30. Found: C, 52.86; H, 3.38; N, 10.42. ESI-MS: *m*/*z* 691 [Cu(FcNP)$_2$]$^{1+}$. IR (KBr, cm^{-1}): ν (FcNP) 1607 (vs) 1553 (m), 1508 (s), 1441 (m), 1144 (m), 1103 (m), 842 (m), 812 (m), 523 (m); ν (NO_3^-) 1470 (s), 1381 (s), 1296 (s). UV−vis (CH_3CN; λ_{max}, nm (log ε)): 221 (4.81), 314 (4.36), 382 (3.74), 471 (3.31).

[Zn(FcNP)$_4$][OTf]$_2$ (3). The reaction of $Zn(O_3SCF_3)_2$ (14 mg, 0.0385 mmol) and FcNP (50 mg, 0.16 mmol) was carried out following a procedure similar to that described for the synthesis of **1**. Yield: 56 mg (90%). Single crystals were grown by layering petroleum ether onto a saturated dichloromethane solution of compound **3** inside an 8 mm o.d. vacuum-sealed glass tube. Anal. calcd for $C_{74}H_{56}N_8O_6F_6S_2Fe_4Zn_1$: C, 54.86; H, 3.48; N, 6.92. Found: C, 54.73; H, 3.36; N, 6.98. ESI-MS: *m*/*z* 661 ($z = 2$) [Zn(FcNP)$_4$]$^{2+}$.

Table 3. Crystallographic Data and Pertinent Refinement Parameters for **1**−**5**, **8**, and **9**

	1·CH_2Cl_2	**2**	**3**·CH_2Cl_2	**4**·$2CH_2Cl_2$	**5**·CH_2Cl_2	**8**	**9**
empirical formula	$C_{37}H_{30}Cl_4Fe_3N_4$	$C_{36}H_{28}CuFe_2N_6O_6$	$C_{75}H_{56}Cl_2F_6Fe_4N_8O_6S_2Zn$	$C_{74}H_{60}B_2CdCl_4F_8Fe_4N_8$	$C_{43}H_{36}Cl_2F\ Fe_2N_4O_{11}Rh_2S_2$	$C_{26}H_{18}Cl_2FeN_4Pd$	$C_{26}H_{18}Cl_2Cu_2FeN_4O_8$
fw	840.00	815.88	1703.07	1712.52	1351.30	619.59	768.27
cryst syst	monoclinic	monoclinic	monoclinic	orthorhombic	monoclinic	monoclinic	monoclinic
space group	$P2_1/c$	$P2_1/n$	$P2_1/c$	$Pbcn$	$P2_1/c$	$C2/c$	$P2_1/c$
a (Å)	13.5633(9)	12.4048(8)	19.249(2)	11.9587(10)	16.7544(13)	19.222(3)	16.4036(11)
b (Å)	27.3844(17)	16.6158(10)	15.8777(18)	25.393(2)	13.9924(11)	10.3762(16)	16.3774(11)
c (Å)	9.3426(6)	15.8849(10)	22.511(3)	22.5542(19)	20.2439(15)	12.950(2)	9.6763(7)
α (deg)	90	90	90	90	90	90	90
β (deg)	103.3960(10)	95.6660(10)	97.129(2)	90	100.6660(10)	117.968(3)	106.1950(10)
γ (deg)	90	90	90	90	90	90	90
V (Å^3)	3375.6(4)	3258.1(4)	6826.8(14)	6848.9(10)	4663.9(6)	2281.2(6)	2496.4(3)
Z	4	4	4	4	4	4	4
ρ_{calcd} (g cm^{-3})	1.653	1.663	1.657	1.661	1.924	1.804	2.044
μ (mm^{-1})	1.624	1.584	1.394	1.362	1.599	1.682	2.540
F(000)	1704	1660	3456	3448	2688	1232	1536
reflns collected	22013	16297	11599	43036	26588	7098	16254
independent reflns	8249	5554	11599	8483	9479	2732	6072
observed reflns [$I > 2\sigma(I)$]	6155	4914	5928	6993	7621	2494	4620
no. of variables	433	460	937	461	576	155	402
GOF	1.058	1.053	0.935	1.057	1.095	1.086	1.049
final R indices [$I > 2\sigma(I)$][a]	$R_1 = 0.0442$ $wR_2 = 0.1009$	$R_1 = 0.0346$ $wR_2 = 0.0792$	$R_1 = 0.0625$ $wR_2 = 0.0912$	$R_1 = 0.0374$ $wR_2 = 0.0831$	$R_1 = 0.0837$ $wR_2 = 0.2007$	$R_1 = 0.0248$ $wR_2 = 0.0639$	$R_1 = 0.0537$ $wR_2 = 0.1168$
R indices (all data)[a]	$R_1 = 0.0656$ $wR_2 = 0.1162$	$R_1 = 0.0399$ $wR_2 = 0.0816$	$R_1 = 0.1464$, $wR_2 = 0.1144$	$R_1 = 0.0521$ $wR_2 = 0.0914$	$R_1 = 0.1021$ $wR_2 = 0.2126$	$R_1 = 0.0286$ $wR_2 = 0.0669$	$R_1 = 0.0774$ $wR_2 = 0.1284$

[a] $R_1 = \sum||F_o| - |F_c||/\sum|F_o|$ with $F_o^2 > 2\sigma(F_o^2)$. $wR_2 = [\sum w(|F_o^2| - |F_c^2|)^2/\sum|F_o^2|^2]^{1/2}$.

IR (KBr, cm^{-1}): ν (FcNP) 1611 (s), 1560 (s), 1509 (s), 1445 (m), 1414 (m), 1146 (s), 1103 (s), 842 (m), 812 (m), 517 (m), 498 (m); ν (OTf$^-$) 1271 (vs), 1030 (s), 636 (s). ^{1}H NMR (CD_3CN, δ): 8.89 (br, 1H, NP), 8.42 (br, 1H, NP), 8.13 (br, 1H, NP), 7.51 (br, 2H, NP), 4.47−4.16 (br, 4H, Fc), 4.09 (br, 5H, Fc). UV−vis (CH_3CN; λ_{max}, nm (log ε)): 221 (4.80), 330 (4.36), 403 (3.56), 512 (3.61).

$[Cd(FcNP)_4][BF_4]_2$ (4). The reaction of $Cd(BF_4)_2$ (12 mg, 0.042 mmol) and FcNP (54 mg, 0.172 mmol) was carried out following a procedure similar to that described for the synthesis of **1**. Yield: 52 mg (80%). Single crystals were grown by the diffusion of petroleum ether onto a dichloromethane solution of the **4** inside an 8 mm o.d. vacuum-sealed glass tube. Anal. calcd for $C_{72}H_{56}N_8B_2F_8Fe_4Cd$: C, 56.06; H, 3.66; N, 7.26. Found: C, 56.04; H, 3.63; N, 7.35. ESI-MS: m/z 685 ($z = 2$) $[Cd(FcNP)_4]^{2+}$. IR (KBr, cm^{-1}): ν (FcNP) 1608 (s), 1557 (m), 1508 (s), 1442 (m), 1415 (s), 1382 (m), 1300 (w), 1285 (w), 1143 (m), 843 (m), 810 (m), 522 (m); ν (BF_4^-)1069 (s). ^{1}H NMR ($CDCl_3$, δ): 9.06 (d, 1H, NP), 8.33 (dd, 1H, NP), 8.09 (d, 1H, NP), 7.56 (br, 2H, NP), 5.23 (d, 2H, Fc), 4.62 (br, 2H, Fc), 4.07 (s, 5H, Fc). UV−vis (CH_3CN; λ_{max}, nm (log ε)): 221 (4.79), 314 (4.33), 390 (sh), 471 (3.25).

$[Rh_2(FcNP)_2(\mu\text{-}O_2CCH_3)_2(H_2O)][OTf]_2$ (5). FcNP (26 mg, 0.083 mmol) was added to a 1,2-dichloroethane solution (20 mL) of $[Rh_2(OAc)_2(MeCN)_6][BF_4]_2$ (29 mg, 0.039 mmol), and the resulting blue solution was stirred for 8 h at room temperature. The solution was concentrated, and 15 mL of diethyl ether was added with stirring to induce precipitation. The resulting blue solid residue was washed with diethyl ether (3 × 10 mL) and dried in a vacuum to give $[Rh_2(FcNP)_2(OAc)_2(H_2O)][BF_4]_2$ (**5a**). Yield: 36 mg (81%). Anal. calcd for $C_{40}H_{36}N_4O_5B_2F_8Fe_2Rh_2$: C, 42.00; H, 3.17; N, 4.90. Found: C, 41.92; H, 3.25; N, 5.21. ESI-MS: m/z 1039 $[Rh_2(FcNP)_2(OAc)_2(BF_4^-)]^+$. IR (KBr, cm^{-1}): ν (OAc$^-$) 1613(s), 1443 (vs); ν (BF_4^-) 1059 (vs); ν (H_2O) 3434 (br, m); ν (FcNP) 1557 (m), 1508(m). ^{1}H NMR (CD_3CN, δ): 10.84 (s, 1H), 9.63 (br, 2H), 8.28−8.16 (m, 3H), 7.94 −7.86 (m, 6H), 7.64−7.57 (m, 3H), 6.26 (s, 1H), 6.06 (s, 2H), 5.44 (s, 3H), 4.99 (d, 3H), 4.77 (m, 5H), 1.58 (br, 1H), 1.33 (m, 3H), 0.95 (m, 3H). UV−vis (CH_3CN; λ_{max}, nm (log ε)): 210 (4.42), 272 (3.94), 347 (3.78), 390 (sh), 564 (3.31). X-ray-quality crystals of $[Rh_2(FcNP)_2(OAc)_2(H_2O)][OTf]_2$ (**5**) were obtained in quantitative yield by layering petroleum ether onto a dichloromethane solution of [n-Bu_4N][OTf] and $[Rh_2(FcNP)_2(OAc)_2(H_2O)][BF_4]_2$ inside an 8 mm o.d. vacuum-sealed glass tube. Anal. calcd for $C_{42}H_{36}N_4S_2F_6O_{11}Fe_2Rh_2$: C, 39.77; H, 2.86; N, 4.42; S, 5.06. Found: C, 39.59; H, 2.77; N, 4.42; S, 4.93. IR (KBr, cm^{-1}): ν (OAc$^-$) 1613(s), 1443(vs); ν (OTf$^-$) 1270 (vs); ν (OH_2) 3434 (br, m).

$[PdCl_2(FcNP_2)]$ (8). $FcNP_2$ (25 mg, 0.0565 mmol) was added to an acetonitrile solution (15 mL) of $PdCl_2(C_6H_5CN)_2$ (20 mg, 0.052 mmol), and the mixture was stirred for 8 h at room temperature. The resulting red precipitate was washed with dichloromethane (2 × 10 mL) and dried under a vacuum to give **8**. Yield: 23 mg (71%). X-ray-quality crystals were grown by layering an acetonitrile solution (5 mL) of $PdCl_2(C_6H_5CN)_2$ (10 mg, 0.026 mmol) onto a methanolic solution (5 mL) of $FcNP_2$ (12 mg, 0.027 mmol) inside an 8 mm o.d. vacuum-sealed glass tube. Anal. calcd for $C_{26}H_{18}N_4Cl_2FePd$: C, 50.40; H, 2.93; N, 9.04. Found: C, 50.53; H, 2.97; N, 9.23. ESI-MS: m/z 583 $[M - Cl]^{1+}$. IR (KBr, cm^{-1}). ν ($FcNP_2$) 1606 (s), 1556 (m), 1509 (s), 1439 (m), 1380 (m), 1136 (m), 1100 (m), 840 (m), 813 (m), 493 (m).

$[Cu_2(FcNP_2)][ClO_4]_2$ (9). An acetonitrile solution (20 mL) of $[Cu(CH_3CN)_4][ClO_4]$ (28 mg, 0.086 mmol) was treated with $FcNP_2$ (18 mg, 0.041 mmol), and the resulting solution was stirred at room temperature for 8 h. The solution was concentrated under a vacuum, and diethyl ether was added to induce complete precipitation. A red solid residue was collected by filtration, washed with CH_2Cl_2, and dried in a vacuum to give compound **9**. X-ray-quality crystals were grown by layering diethyl ether onto a nitromethane solution of **9** inside an 8 mm o.d. vacuum-sealed glass tube. Yield: 60 mg (91%). Anal. calcd for $C_{26}H_{18}N_4O_8Cl_2Cu_2Fe_1$: C, 40.65; H, 2.36; N, 7.29. Found: C, 40.47; H, 2.29; N, 7.38. ESI-MS: m/z 505

(38) Software for CCD difractometers: *SAINT*+; Bruker AXS: Madison, WI, 2000.

$[Cu(FcNP_2)]^+$, 669 $[\{Cu_2(FcNP_2)\}^{2+} + ClO_4^-]^+$. IR (KBr, cm^{-1}): ν ($FcNP_2$) 1607 (m), 1560 (w), 1510 (m), 1441 (w), 1381 (w), 488 (w) ν (ClO_4^-) 1142 (s), 1087 (vs).

Conversion of $[\{Cu(FcNP_2)\}_2][ClO_4]_2$ (6) to $[Cu_2(FcNP_2)][ClO_4]_2$ (9). A nitromethane solution (15 mL) of **6** (40 mg, 0.033 mmol) was treated with an acetonitrile solution of 2 equiv of $[Cu(CH_3CN)_4][ClO_4]$ (22 mg, 0.067 mmol), and the solution was stirred for 4 h at room temperature. The resulting solution was concentrated, and diethyl ether was added to induce precipitation. The solid residue was filtered, washed with dichloromethane, and dried in a vacuum. Yield: 45 mg (90%).

Conversion of $[Cu_2(FcNP_2)][ClO_4]_2$ (9) to $[\{Cu(FcNP_2)\}_2][ClO_4]_2$ (6). A nitromethane solution (15 mL) of **9** (40 mg, 0.052 mmol) was treated with 1 equiv of the $FcNP_2$ ligand (25 mg, 0.056 mmol), and the solution was stirred for 6 h at room temperature. The resulting solution was concentrated, and diethyl ether was added to induce precipitation. The solid residue was filtered, washed with dichloromethane, and dried in a vacuum. Yield: 54 mg (86%).

X-Ray Data Collection and Refinement. Single-crystal X-ray studies were performed on a CCD Bruker SMART APEX diffractometer equipped with an Oxford Instruments low-temperature attachment. Data for **8** were collected at room temperature (298 K), whereas other data were collected at 100(2) K using graphite-monochromated Mo Kα radiation ($\lambda_\alpha = 0.71073$ Å). The frames were indexed, integrated, and scaled using the SMART and SAINT software packages,[38] and the data were corrected for absorption using the SADABS programs.[39] Structures were solved and refined with the SHELX suite of programs[40] as implemented in X-seed,[41] while additional crystallographic calculations were performed by the program PLATON.[42] The figures were drawn using ORTEP32.[43] The hydrogen atoms were included at geometrically calculated positions in the final stages of the refinement and were refined according to the "riding model". All non-hydrogen atoms were refined with anisotropic thermal parameters unless mentioned otherwise. Pertinent crystallographic data for compounds **1**−**5**, **8**, and **9** are summarized in Table 3.

An empirical absorption correction was applied for compound **3** using XABS2.[44] The dichloromethane solvate molecule in **3** was found to be disordered and was modeled satisfactorily. The disordered C atoms were refined isotropically. In compound **4**, the disordered dichloromethane solvate was modeled satisfactorily. The disordered triflate anions in **5** were modeled with restrained parameters. The S atoms were refined anisotropically, while other constituting atoms (C, F, and O) were refined isotropically. The oxygen atom of the axially coordinated water molecule was refined isotropically. One of the perchlorate anions in **9** was found to be severely disordered and was modeled with restrictions. Structure solution and refinement details are provided in the Supporting Information.

Acknowledgment. Authors thank Dr. Sanjib. K. Patra for his contribution to this work. Financial supports from the DST, India, and CSIR, India, for this research is gratefully acknowledged. Our special thanks to the DST for the ESI-MS facility at IIT Kanpur through the FIST program. N.S. thanks the CSIR for a fellowship.

Supporting Information Available: X-ray crystallographic data in CIF format; details of X-ray data collection and refinement; tables of bond distances and angles for **1**−**5**, **8** and **9**; thermal ellipsoid diagrams for FcNP, **1**−**5**, **8** and **9**; measured and calculated ESI-MS spectra of compounds **1**−**9**; cyclic voltammograms of FcNP, $FcNP_2$, **5**, and **9**; and absorption and emission spectra of FcNP and **1**−**5** in the solution state and solid state excitation and emission spectra of $FcNP_2$ and **6**−**10** along with a table of electronic and photophysical spectral data; crystal packing diagrams of $FcNP_2$, **1**−**6** and **8**. This material is available free of charge via the Internet at http://pubs.acs.org.

IC801586D

(39) Sheldrick, G. M. Program for Correction of Area Detector Data: *SADABS*; University of Göttingen: Göttingen, Germany, 1999.

(40) (a) *SHELXTL*, version 6.10; Bruker AXS: Madison, WI, 2000. (b) Sheldrick, G. M. *SHELXS-86*; *SHELXL-97*; University of Göttingen: Göttingen, Germany, 1997.

(41) (a) Atwood, J. L.; Barbour, L. J. *Cryst. Growth Des.* **2003**, *3*, 3. (b) Barbour, L. J. *J. Supramol. Chem.* **2001**, *1*, 189.

(42) Spek, L. *PLATON*; University of Utrecht: Utrecht, The Netherlands, 2001.

(43) Farrugia, L. J. *J. Appl. Crystallogr.* **1997**, *30*, 565.

(44) Parkin, S. R.; Moezzi, B.; Hope, H. *J. Appl. Crystallogr.* **1995**, *28*, 53.